NONLINEAR AXISYMMETRIC LIQUID CURRENTS IN SPHERICAL ANNULII

N. M. Astaf'yeva, N. D. Vvedenskaya, and I. M. Yavorskaya

Translation of Nelineynyye Osesimmetrichnyye Techeniya Zhidkosti v Sfericheskikh Sloyak, Academy of Sciences USSR, Institute of Space Research, Moscow, Report-385, 1978, pp. 1-55

(NASA-TM-75559) NONLINEAR AXISYMMETRIC LIQUID CURRENTS IN SPHERICAL ANNULI (National Aeronautics and Space Administration) 55 p HC A04/MF A01 CSCL 20D

N79-10376

Unclas
G3/34 33898

NATIONAL AERONAUTICS AND SPACE ADMINISTRATION
WASHINGTON, D.C. 20546 OCTOBER 1978

STANDARD TITLE PAGE

1. Report No.
NASA-TM-75559

2. Government Accession No.

3. Recipient's Catalog No.

4. Title and Subtitle
NONLINEAR AXISYMMETRIC LIQUID CURRENTS IN SPHERICAL ANNULII

5. Report Date
October 1978

6. Performing Organization Code

7. Author(s)
N. M. Astaf'yeva, N. D. Vvedenskaya, and I. M. Yavorskaya

8. Performing Organization Report No.

10. Work Unit No.

9. Performing Organization Name and Address
SCITRAN
Box 5456
Santa Barbara, CA 93108

11. Contract or Grant No.
NASW-3198

13. Type of Report and Period Covered
Translation

12. Sponsoring Agency Name and Address
National Aeronautics and Space Administration
Washington, D.C. 20546

14. Sponsoring Agency Code

15. Supplementary Notes
Translation of Nelineynyye Osesimmetrichnyye Techeniya Zhidkosti v Sfericheskikh Sloyak, Academy of Sciences USSR, Institute of Space Research, Moscow, Report-385, 1978, pp. 1-55.

16. Abstract
A numerical analysis of non-linear axysimmetric viscous flows in spherical annulii of different gap sizes is presented. Only inner sphere was supposed to rotate at a constant angular velocity.

The streamlines, lines of constant angular velocity, kinetic energy spectra and spectra of velocity components are obtained. A total kinetic enrgy and torque needed to rotate the inner sphere are calculated as functions of R_e for different gap sizes.

In small-gap annulus non-uniqueness of steady solutions of N.-St. equations is established and regions (in R_e) of different flow régime existances are found.

Numerical solutions in a wide-gap annulus together with experimental results permit to conclude the flow stability in considered range of R_e.

The comparison of experimental and numerical results shows the close not only qualitative but quantitative agreement.

17. Key Words (Selected by Author(s))

18. Distribution Statement
Unclassified - Unlimited

19. Security Classif. (of this report)
Unclassified

20. Security Classif. (of this page)
Unclassified

21. No. of Pages

22.

TABLE OF CONTENTS

ANNOTATION

We present a numerical analysis of nonlinear axisymmetric currents in a viscous liquid in spherical annulii of various thickness when only the inner sphere rotates.

We obtained the lines of flow and the lines of equal angular velocity, the spatial spectra of the kinetic energy and of individual velocity components; we calculated the integral characteristics of the motions: the total kinetic energy and the torque for various values of the numbers Re.

In a thin annulus, the nonuniqueness of the steady-state solutions of the Navier-Stokes equations was established, and the regions (with respect to Re) in which various flow regimes exist were determined.

Calculations of the currents in a thick annulus together with the results of previous experiments make it possible to draw conclusions concerning the stability of currents in the Re range considered.

Comparison of the numerical results with experiments shows good quantitative and qualitative agreement.

Nonlinear Axisymmetric Liquid Currents in Spherical Annulii

N. M. Astaf'yeva, N. D. Vvedenskaya, and I. M. Yavorskaya

INTRODUCTION

The study of nonlinear shearing currents in a liquid or a gas in rotating spherical annulus is the basis for an understanding of many dynamic processes of global scale in oceans, the atmospheres of the Earth, planets, and in the interior of stars of various spectral classes. /5*

In all these instances, the form of the currents and their stability depends essentially on two important factors: the spherical geometry of the volume in which they flow, and the rotation. Neglect of even one of these factors can lead to results quite remote from reality, as experiments show [1 - 6].

One of the simplest shearing currents in which such factors are considered is a current in a viscous incompressible liquid in a spherical annulus, the boundaries of which rotate around the same axis with different constant angular velocities. By analogy with the plane and cylindrical cases, we call it the Couette spherical current.

The published results of experiments [1 - 6] have shown that, depending on the values of the parameters of similar problems: the Reynolds number $Re = (\Omega_1 r_1^2)/\nu$, the relative thickness of the

*Numbers in the margin indicate pagination in the original foreign text.

annulus $\delta = \frac{r_2 - r_1}{r_1}$, and the Rossby number $\varepsilon = \frac{\Omega_2 - \Omega_1}{\Omega_1}$ (or the Reynolds number with respect to the external sphere $Re_2 = \frac{\Omega_2 r_2^2}{\nu}$), /6 the character and form of the currents arising in the annulus turn out to be extraordinarily diverse (r_1, r_2, Ω_1 and Ω_2 are the radii and the angular velocities of rotation of the internal and external spheres, respectively, and ν is the kinematic viscosity).

For sufficiently small numbers Re [7 - 10], the Couette spherical current is axisymmetric and consists of differential rotations around the axis and the meridional circulation whose intensity and form for fixed numbers Re are determined by the parameters δ and ε. Here it is already clear that the analogy between the plane and cylindrical currents, on the one hand, and the spherical, on the other, is purely external: the first two currents are one-dimensional and have one velocity component in the direction of the displacement of the velocity. A current in a spherical annulus is much more complex: it has three velocity components and depends on the two spherical coordinates r and θ, and on the Reynolds number.

This difference becomes still more significant when the basic current loses stability. In the plane case, if the very first instability leads to the spontaneous development of turbulence and, in the cylindrical case, to the appearance of stationary axisymmetric or (when the Rossby numbers are large and negative) periodic undulating Taylor vortices, then in the spherical annulus [5, 11] when the basic current loses stability, there arise diverse currents which differ widely among themselves, depending on the thickness of the annulus and the number ε. Obviously this indicates that there are various mechanisms which cause the instability of the basic current for different δ and ε.

Such a difference between plane, cylindrical and spherical currents arouses not only applied, but also theoretical interest in the study of Couette spherical currents, since they obviously are more general in character. This greater generality leads, as is to be expected, to significantly greater mathematical difficulties in obtaining a solution: indeed, for arbitrary values of similar parameters, calculation of the spherical current reduces to the solution of a boundary value problem for a system of nonlinear partial differential equations. /7

It is possible, therefore, that the most interesting results were those obtained experimentally in recent years. The analytical and numerical results are few in number and relate only to certain specific points in the space of similar parameters. A detailed analysis of all results in papers published up to 1974 is given in our survey article [12]. Here we shall touch on only those results in recent years, of which our paper is a direct development.

First of all, let us note that spherical annulii can be subdivided into thin annulii where $\delta < \delta^*$, and thick annulii with $\delta > \delta^*$, depending on whether or not the principle of "change of stability" holds at the limit of stability when $Re = Re_c$. The critical value of the Reynolds number is a function of δ and ε, and the critical value of the thickness of the annulli δ^*, for which the character of the secondary current changes also, is obviously a function of the Rossby number ε. Henceforth, we shall consider only rotations of the internal sphere for which $\delta^* = 0.24$.

Up the the present, the question as to the stability of the Couette spherical current in thick annulii has not been resolved unambiguously. For a long time it was assumed that thick annulii were always stable [1, 2, 13]. The fact which the energy theory [10] of the qualitative difference between thick and thin shells did not discover is that the lower boundary of the limit of stability in thick annulii was somewhat higher than in thin annulii. According to this theory, the most dangerous disturbances for all δ and ε turned out to be the nonaxisymmetrical distrubances with azimuthal wave number $m = 1$.

The most detailed experiments have shown, however, that thick annulii are also unstable. In the papers [3, 6], the authors demonstrated visually the loss of stability by currents in annulii of thickness $0{,}24 \leq \delta \leq 1$ for $Re_c = Re_c(\delta)$, significantly exceeding the critical values of Re_E from the energy theory and exceeding the anticipated critical values obtained by extrapolation from the experimental stability curve in thin annulii. At the limit of stability, a complex secondary nonaxisymmetrical current was observed, consisting of the same number of vortices in each hemisphere and propagated in an azimuthal direction at a certain phase velocity $\Omega(\delta) < \Omega_1$. /8

A completely different result was obtain in [4], where the stability of the currents in thick annulii with $\delta = 1{,}27$ and 2.25 were studied by measuring the torque M transmitted to the external sphere, and by visual means. On the curve M = M(Re), four breaks were found in the current in the annulus with $\delta = 1{,}27$, the first three when the numbers $Re_{c1} < Re_{c2} < Re_{c3}$ were smaller than $Re_c(\delta = 1{,}33)$ (obtained in [6, 11]), and only the fourth break occurred when $Re_{c4} \approx Re_c$ ($\delta = 1{,}33$). Usually, breaks in the integral characteristics of the currents correspond to the onset of instability and the emergence of a secondary current visually distinct from the pre-critical current. Visually, no significant rearrangements of the current were detected for the first three breaks; the fourth break, corresponding to $Re_c(\delta = 1{,}33)$ of [11], was identified with a sudden complete turbulization of the flow. In [4] it was proposed that for Re_{c1} the first break corresponds to a drastic instability of the basic current of finite amplitude, which leads to secondary currents of the same form as the basic current.

Additional experiments conducted by us [11] in a thick annulus with $\delta = 1{,}33$ with the help of the film thermal flowmeter "DISA" /9 mounted in the equatorial plane of the current, have shown that there are no changes in the characteristics of the current up to the values $Re_{c_4} = Re_c$. When $Re > Re_c$ the recorded signal, its spectral density and the correlation function have shown the presence of only one frequency of the visually observed vortices. Moreover, investigation of the spectral characteristics of the current for the highly supercritical numbers $Re \approx 2\, Re_c$ have also shown that there are in the current no more than two different oscillation frequencies. Thus it was established that the transition through $Re = Re_c$, corresponding to the fourth break, is not accompanied by the sudden emergence of turbulence, but by the transition to a complex stratified periodic motion such as may be found in [3]. The question regarding the first three breaks remained open, since the change to a steady-state regime established with the aid of a thermal flowmeter is much more complicated.

To clarify this question in the present paper, numerical investigations of liquid currents were undertaken in an annulus of thickness $\delta = 1,33$ in the interval $0 \leq Re \leq 250$, the results of which are disucssed in sections 2 and 3. We obtained curves of the torque and the kinetic energy as functions of the Reynolds number, and we studied the structure and scale of the prevailing motions.

Previous numerical investigations of the currents in a thick annulus ($\delta = 1$) were presented in [7 - 10]. However, the form in which these results were presented and the small number of them made them unsuitable for our purposes.

In thin annulii with $\delta < 0,24$ in the supercritical region, it was discovered experimentally that there exist several steady-state axisymmetric current regimes [2, 4 - 6, 14, 15] such that some of them can exist for the same number Re, depending on the prehistory /10
of the process — which agrees with the nonuniqueness of the solution of the steady-state boundary problem for the Navier-Stokes equations. In particular, it was established experimentally that

in an annulus with thickness $\delta = 0,II$, there exist 4 steady-state currents with two, four, six, and eight annular vortices, parallel to the equator [6].

In the present paper, we study numerically all the experimentally obtained nonlinear steady-state axisymmetric currents in an annulus of $\delta = 0,II$; we establish the limits of their existence and the possible transitions from one regime to another. In contrast to the experiment, numerical modeling made it possible to study the structure of the currents, their energy characteristics, and the linear scale of the prevalent motions, etc.

We know of only one paper [14] in which the authors discuss the results of separate calculations for the flow functions of the currents when $\mathcal{E} = -I$ in thin annulii with $\delta = 0,I76$ for Re = 700, 900, and 1500 and with $\delta = 0,9375$, $Re = 3000 - 8000$ without any analysis of the sequential transitions of the various regimes and the regions of existence and nonuniqueness of the currents.

We present the results of calculations of the currents in a liquid in a thin and a thick annulus during rotation of the internal sphere only; the physical interpretation of the results and a comparison with experiment are discussed later in sections 2 and 3.

1. STATEMENT OF THE PROBLEM AND THE METHOD OF SOLUTION

The Couette spherical current is described mathematically by the solution of the boundary value problem for the Navier-Stokes system of equations. We shall find the steady-state solution by the method of adjustment, i.e., as the limit (if it exists) when $t \to \infty$ of the solution of the initial-boundary value problem for the nonsteady-state equations (t is time). In dimensionless form, the problem has the form: /11

$$\frac{\partial \vec{u}}{\partial t} + (\vec{u}\nabla)\vec{u} = -\nabla p + \frac{1}{Re}\Delta\vec{u}, \tag{2.1}$$

$$\operatorname{div}\vec{u} = 0,$$

$$\begin{array}{ll} u_r = u_\theta = 0, \; u_\varphi = \sin\theta; & \text{when } r = 1, \\ u_r = u_\theta = 0, \; u_\varphi = \omega(1+\delta)\sin\theta. & \text{when } r = 1+\delta, \end{array} \tag{2.2}$$

$$u_r\Big|_{t=0} = u_r^0, \; u_\theta\Big|_{t=0} = u_\theta^0, \; u_\varphi\Big|_{t=0} = u_\varphi^0. \tag{2.3}$$

here, $\bar{u}$ is the velocity vector; p is the pressure; u_r, u_θ, u_φ are the components of $\bar{u}$ in spherical coordinates r, θ, φ. For the scales of length, time, velocity and pressure, we assume, respectively, the radius of the internal sphere r_1, the reciprocal of the angular rotational velocity of the internal sphere Ω_1^{-1}, $\Omega_1 r_1$ and $\rho_0\Omega_1 r_1^2$ (ρ_0 is the density of the liquid), $\omega = \Omega_2/\Omega_1 = \varepsilon + 1$.

For the numerical solution of the problem, we shall follow the procedure in [16].

We seen an axisymmetrical solution of (2.1) - (2.3). Let us represent the desired functions in the form of a series in terms of the associated functions $\mathcal{P}_e^0(x)$ and $\mathcal{P}_e^1(x)$, where $x = \cos\theta$, and the coefficients depend on r and t. We shall restrict ourselves to a finite number of terms in the series:

$$\begin{aligned} u_r(r,\theta,t) &= \sum_{\ell=0}^{L} U_\ell(r,t)\mathcal{P}_\ell^0(x); \quad p(r,\theta,t) = \sum_{\ell=0}^{L} P_\ell(r,t)\mathcal{P}_\ell^0(x), \\ u_\theta(r,\theta,t) &= \sum_{\ell=1}^{L} V_\ell(r,t)\mathcal{P}_\ell^1(x), \\ u_\varphi(r,\theta,t) &= \sum_{\ell=1}^{L} W_\ell(r,t)\mathcal{P}_\ell^1(x) + \omega r\mathcal{P}_1^1(x): \end{aligned} \tag{2.4}$$

Here in U_φ, the term $\overset{\circ}{\omega} r \mathcal{P}_1^1(x)$ which is isolated in the steady-state solution of (2.1) - (2.2) when $Re \to 0$ (the Stokes current). For this term we have:

$$\overset{\circ}{\omega} = 1 + \alpha\left(1 - \frac{1}{r^3}\right) \;;\; \alpha = (\omega - 1)\frac{(1+\delta)^3}{(1+\delta)^3 - 1}$$

Let us represent the nonlinear terms in analogous form [for brevity all calculations are hereafter presented much as the first of the equations (2.1)]:

$$\mathcal{F}_1(r,\theta,t) = -\left\{U_r\frac{\partial U_r}{\partial r} + \frac{U_\theta}{r}\frac{\partial U_r}{\partial \theta} - \frac{U_\theta^2 + U_\varphi^2}{r}\right\} =$$
$$= -\left\{\sum_{\ell=0}^{L} U_\ell \mathcal{P}_\ell^0 \sum_{\ell=0}^{L} \frac{\partial U_\ell}{\partial r}\mathcal{P}_\ell^0 + \right.$$
$$+ \frac{1}{r}\sum_{\ell=1}^{L} V_\ell \mathcal{P}_\ell^1 \sum_{\ell=1}^{L} U_\ell \mathcal{P}_\ell^1 - \frac{1}{r}\left(\sum_{\ell=1}^{L} V_\ell \mathcal{P}_\ell^1\right)^2 -$$
$$\left. - \frac{1}{r}\left(\sum_{\ell=1}^{L} W_\ell \mathcal{P}_\ell^1 + \overset{\circ}{\omega} r \mathcal{P}_1^1\right)^2\right\}. \qquad (2.5)$$

$$\mathcal{F}_1(r,\theta,t) = \sum_{\ell=0}^{L} \Phi_{1,\ell}(r,t)\,\mathcal{P}_\ell^0,$$
$$\mathcal{F}_i(r,\theta,t) = \sum_{\ell=1}^{L} \Phi_{i,\ell}(r,t)\,\mathcal{P}_\ell^0, \; i = 2, 3.$$

Let us especially stress the choice of the method of approximating the terms $\mathcal{F}_i$, $i = 1, 2, 3$. We shall consider our expansions as interpolationsal, i.e., we shall require that the equations (2.5) be satisfied for $\theta = \theta_j \;, j = 0, \ldots, L$, where $\theta_j \doteq j\frac{\pi}{L}$.

Such a choice of θ_j is explained by the fact that it is natural to treat our functions like the function $x = \cos\theta$, $-1 \le x \le 1$, and the points $x_j = \cos\theta_j$ are here the zeros of a Chebyshev polynomial. It is well-known that interpolation with /13
respect to such a system of nodes is optimal in some sense.

Substituting (2.4) and (2.5) into (2.1), we may now separate the variables, and obtain for $U_\ell, V_\ell, W_\ell, P_\ell$ the following system of equations:

$$
\begin{aligned}
&\frac{\partial U_\ell}{\partial t} - \frac{1}{Re}\left\{\frac{1}{r^2}\frac{\partial}{\partial r} r^2 \frac{\partial U_\ell}{\partial r} + \frac{2}{r}\frac{\partial U_\ell}{\partial r} + \frac{2-\ell(\ell+1)}{r^2} U_\ell\right\} + \\
&\qquad + \frac{\partial P_\ell}{\partial r} = \phi_{1,\ell}, \\
&\frac{\partial V_\ell}{\partial t} - \frac{1}{Re}\left\{\frac{1}{r^2}\frac{\partial}{\partial r} r^2 \frac{\partial V_\ell}{\partial r} - \frac{\ell(\ell+1)}{r^2} V_\ell + \frac{2}{r^2} U_\ell\right\} + \\
&\qquad + \frac{P_\ell}{r} = \phi_{2,\ell}, \\
&\frac{\partial W_\ell}{\partial t} - \frac{1}{Re}\left\{\frac{1}{r^2}\frac{\partial}{\partial r} r^2 \frac{\partial W_\ell}{\partial r} - \frac{\ell(\ell+1)}{r^2} W_\ell\right\} = \phi_{3,\ell}, \\
&\frac{1}{r^2}\frac{\partial}{\partial r} r^2 U_\ell - \frac{\ell(\ell+1)}{r} V_\ell = 0.
\end{aligned}
\tag{2.6}
$$

The boundary conditions assume the form:

$$
U_\ell(r,t) = V_\ell(r,t) = W_\ell(r,t) = 0 \text{ for } r = 1;\ 1+\delta. \tag{2.7}
$$

It is clear that equations (2.5) are exactly satisfied on the rays:

$$
\theta = \theta_j \quad ; \quad j = 0, \ldots, L.
$$

Let us now carry out the discretization of the problem with respect to t and r and pass from (2.6) to finite difference equations. As a preliminary step, let us make a change in the independent variable r by means of the formulas $s = f(r)$, so that, after obtaining the equally spaced points of the difference scheme, the calculated points could be obtained which are not equally spaced relative to r.

Thus, we shall consider all the functions only at the moment $t_n = n\tau$, $n = 0, 1, \dots$ and at the points $s_k = f(1) + kh$, /14
$k = 0, 1, \dots, K$, or at the points $s_{k+1/2} = f(1) + (k+\frac{1}{2})h$, $k = 0, 1, \dots, K-1$. The functions U_ℓ, V_ℓ, W_ℓ will be given at the points s_k, and P_ℓ at the points $s_{k+1/2}$. Let $g(t_n, s_j) = g^n(j)$. The finite difference equations have the form:

$$\begin{aligned}
&\frac{U_\ell^{n+1}(k)}{\tau} - \frac{1}{Re}\Big\{\left(f'(k)\right)^2 \frac{U_\ell^{n+1}(k+1) - 2U_\ell^{n+1}(k) + U_\ell^{n+1}(k-1)}{h^2} + \\
&+ \left[f''(k) + \frac{4f'(k)}{r(k)}\right] \frac{U_\ell^{n+1}(k+1) - U_\ell^{n+1}(k-1)}{2h} + \\
&+ \frac{2 - \ell(\ell+1)}{(r(k))^2} U_\ell^{n+1}(k)\Big\} + f'(k)\, \frac{P_\ell^{n+1}(k+1/2) - P_\ell^{n+1}(k-1/2)}{h} = \\
&= \Phi_{1,\ell}^{n}(k) + \frac{U_\ell^{n}(k)}{\tau}.
\end{aligned} \tag{2.8}$$

Here, $\Phi_{1,\ell}^{n}(k)$ is the ℓth coordinate in the expansion for $F_1(r,\theta,t)$.

$$U_r^n(k)\,\frac{U_r^n(k+1) - U_r^n(k-1)}{2h}\, f'(k) + \frac{U_\varphi^n(k)}{r(k)}\,\frac{\partial U_r^n(k)}{\partial\theta} - \frac{\left(U_\theta^n(k)\right)^2 + \left(U_\varphi^n(k)\right)^2}{r(k)}.$$

The boundary conditions for (2.8):

$$U_\ell^n(0) = V_\ell^n(0) = W_\ell^n(0) = U_\ell^n(\mathcal{K}) = V_\ell^n(\mathcal{K}) = W_\ell^n(\mathcal{K}) = 0. \quad (2.9)$$

Here,

$$\mathcal{K} = [\, s(1+\delta) - s(\delta) \,] / h$$

everywhere.

It should be emphasized that in (2.8) the linear terms are computed on the $(n+1)^{st}$ annulus, and the nonlinear right side pertains to the h^{th} annulus, so that on each new annulus a linear boundary value problem is solved.

We shall consider only the current which is symmetric with respect to the equator $\theta = \pi/2$; therefore, in the expansion (2.4) is is sufficient to restrict ourselves to the terms of corresponding parity. Namely,

$$u_r = \sum_{\ell=0,2}^{L-1} U_\ell \mathcal{P}_\ell^0 \;; \quad p = \sum_{\ell=0,2}^{L-1} P_\ell \mathcal{P}_\ell^0,$$

$$u_\theta = \sum_{\ell=2,4}^{L-1} V_\ell \mathcal{P}_\ell^1 \;; \quad u_\varphi = \sum_{\ell=1,3}^{L-2} W_\ell \mathcal{P}_\ell^1 + \omega r \mathcal{P}_1^1.$$

In the calculations, L is odd. The equations must be satisfied on $\frac{L+1}{2}$ rays: /15

$$\theta = \theta_j = j\frac{\pi}{L} \quad , \; j = 0, 1, \ldots, \frac{L-1}{2}.$$

(The choice of even L is inconvenient, since in this case the system (2.6) has an additional degeneracy for $\ell = L$). The values of L for various versions are specified in section 2.

The choice of any even step with respect to t requires a certain accuracy; since our scheme is "explicit-implicit", the inertial terms in it are calculated on the lower annulus. The estimate from above for τ which guarantees the stability of the scheme is obtained without difficulty in case the coefficients in (2.8) do not depend on k. It has the form:

$$\tau < C \max|\bar{u}|^2/Re,$$

where $C \sim 1$. In the case of variable coefficients, the character of the estimate is preserved, but varies somewhat. For values of τ in our calculations, cf. the supplement.

While establishing the solutions with respect to time, we varied the torque transmitted to the external sphere:

$$M = M_0 / \frac{8}{3}\pi r_1^3 \Omega_1 \mu = \left[\frac{\partial w_1(r,t)}{\partial r} - \frac{w_1(r,t)}{r}\right]_{r=1},$$

and the kinetic energy of the current:

$$E = \pi \int_0^{\pi} \int_1^{1+\delta} (u_r^2 + u_\varphi^2 + u_\theta^2)\, r^2 \sin\theta \, dr \, d\theta.$$

This was necessary so that these integral characteristics may be maintained with a precision of up to 0.1%. /16

2. RESULTS OF THE NUMERICAL CALCULATIONS

Calculations of the boundary value problem for the Navier-stokes equation in a thick annulus with $\delta = 1,33$, when only the internal sphere was rotated, were carried out in the interval Re: $5 \leq Re \leq 130$ in five steps relative to Re; close to the values Re_{c1} and Re_{c2}, the steps relative to Re were reduced to two. In addition, the current was calculated for Re = 150, 200, and 250. For the initial data, we usually took the values of the functions for the preceding step relative to Re. An example of the calculation for Re = 200 is given in Figure 1.

In all the intervals of the Re values considered, a unique steady-state axisymmetric current was obtained. To verify the uniqueness of the solution, calculations with different initial data were performed. Thus, for example when $Re = 60 > Re_{c_1} \approx 55$ disturbances were introduced into the basic current computed for $L = 31$, disturbances which substantially change the scale of the prevailing motions: 1) the amplitudes of all harmonics, beginning with $\ell \geq 8$, were significantly increased, and for $\ell < 8$, they remained unchanged; 2) the amplitudes of the harmonics with $\ell \leq 4$ were equated to zero, and with $\ell \geq 6$, they increased significantly.

In all cases, the solution was quickly established for the basic regime.

In proportion to the growth in the Reynolds number, the number of associated functions L, used during the calculations, increased. Simultaneously with the characteristics of the current, the spectra of the kinetic energy and the individual components of the velocity were calculated, depending on the meridional wave number ℓ. The spectra made it possible to determine the order of the neglected terms, and thus to evaluate the accuracy with which the solution is approximated by the finite series (2.4).

Since for Re = 60, it turns out to be sufficient to take L = 17, /17
and for Re = 150 to set L = 25, so that the kinetic energy of the neglected terms does not exceed 0.1% of the total kinetic energy of the current. Simultaneously with the calculation of the structure of the current, the integral characteristics were calcualted: the torque transmitted to the external sphere M (Figure 2), and the total kinetic energy E as a function of Re (Figure 3).

In a thin annulus, numerous calculations of the current were carried out from Re = 300 to Re $\lesssim$ 2600. The concrete values of Re for which solutions were obtained are marked with dashes on the diagram (Figure 4). Usually when making the calculations, we took for the initial data the values of the current characteristics for the preceding step relative to Re, the step relative to Re being chosen positive as well as negative.

One of the basic questions in the case of numerical calculations by the direct as well as the semi-direct methods is the question concerning the number of terms retained in the series (2.4). The general notions concerning the increase in L as Re increases are of little help, as we shall see subsequently. To clarify this question for several values of Re, experimental calculations of the currents were performed for various values of L from II to III; the results of the calculations for Re = 1300 and 1500 in the form of the spectral component of the current velocity with respect to ℓ for various values of L are presented in Figures 5 and 6.

The difficulty in choosing L, as is clear from Figures 5 and 6, is due to the fact that in critical situations (loss of stability of the basic current), the spectrum drops rapidly when $L \geq 10$, so that nothing is determined. Indeed, when Re = 1300, the spectra of the r-component of the velocity when L = 11, 21, and 31 are practically identical, and the order of the next terms neglected does not exceed 1% of the maximum value. However, as the calculations with L = 39, 63, 75, and 91 have shown, the actual spectrum has little in common with the spectrum for small L. The point is, as experiment /18 shows, that near this value of Re the basic current becomes unstable, the emerging secondary current has a substantially smaller characteristic linear dimension, and in the spectrum of the meridional component there appears a second maximum for large wave numbers, the prediction of whose occurrence on the basis of calculations with $L < 30$ turned out to be impossible. The spectrum of the r-component changed qualitatively with the increase in L, and the kinetic energy included in the radial component of the motions is now contained not only in the large scale motions of maximum size with $\ell = 2$, but also in the small scale motions with wave numbers $\ell \approx 30$ to 46, i.e., for a sufficiently accurate description of the current when Re $\approx$ 1300, it is necessary to take $\ell \approx 60$.

Thus, to obtain a real picture of the current beyond the limit of stability ($Re_c < Re = 1300$), it is necessary to increase the number of terms of the series more than three-fold. At the same time, to describe the current when Re < 1300 it is sufficient, as calculations showed, to take L = 11. It must be emphasized that five terms of the series (2.4) give smooth, rapidly determined solutions of the equations even for very large Re (calculations performed up to Re = 3000) when, as is familiar from experiment, [5, 6], not a single stability limit is traversed and the basic current simply does not exist, and the ratio of the energy of several of the first neglected terms to the total energy does not exceed the order of several percent.

As the spectrum of U_ℓ shows for Re = 1500 (Figure 6), the qualitative picture of the current is easily discerned when L = 61; when L = 75, 91, 111, the spectral characteristics of the current practically coincide.

As noted above, reorganization of the solution was observed when Re > 1300, and the current emerging here corresponded to the formation near the equator of four annular axisymmetric vortices (Figures 7a, 8a, 9a). This solution exists up to Re = 2200; when the number Re increases further, there occurs a further reorganization of the current, as a result of which another secondary current emerges with eight annular vortices parallel to the equation (Figures 9c, 9c). The solution with 8 vortices exists in our calculations in the interval 1750 ≤ Re ≤ 2600; when Re = 2700, a solution did not appear for a steady-state regime, and an oscillating periodic regime was established with period approximately equal to the period of the single rotation of the sphere. The cause of such oscillations is under study. /19

Henceforth for brevity in diagram 4, and from time to time in the text, we shall use the following designations for the current regimes: we shall designate the current with 2i steady-state annular vortices the regime i (i = 1, 2, 3, 4), and we shall call the basic current the regime 0; the transition from one regime to another will be indicated by arrows.

When Re decreased from 1700, the number of annular vortices in regime 4 decreased to 6 (Figures 7b, 8b, 9b). The regime 3 thus obtained exists "up" to Re = 2700, where it — like regime 4 — becomes oscillatory.

For decreasing Re when Re = 1550, regime 3 goes over into regime 2, and when Re decreases still more, it become regime 0 (for Re = 1300), by-passing regime 1.

To obtain a solution with two annular vortices (regime 1) which, as was known from experiment, arise when Re $\geqq$ 1212 ± 25 during loss of stability by the basic current [6], a special disturbance is introduced into the basic current whose form is close to that of the desired current. In Figures 7c, 10, and 11, the function of the flow and the values of the angular velocity on the surface r = 1.049 are shown, as are also the spectral characteristics of /20 the azimuthal and meridional motions for two different current regimes (regimes 0 and 1) for the same Re = 1270, calculated for the same number of spherical functions L = 91.

Regime 1 exists in the interval 1260 < Re $\leq$ 1400; for larger values of Re, the current is reorganized into the regime with four annular vortices, previously described (regime 2). When Re = 1260, the regime is reorganized into the basic current.

Besides the flow functions and the angular velocity of rotation, spatial spectra of the total kinetic energy and the individual components of the velocity were obtained. In Figure 10 - 19, the graphs of the change in the flow functions and the angular velocity with respect to θ are shown in the center of the annulus when r = 1.049; also included are the Fourier coefficients, U_ℓ, W_ℓ of the the meridional and azimuthal component of the velocity for various regimes of the current when Re = 1270, 1600, 1900, and 2000. In Figure 20, the flow lines and a photograph of regime 4 when Re = 1900 are shown. The spectra of the total kinetic energy for all regimes for Re = 1270, 1600, 1900, and 2200 are presented in Figures 21 - 22. An anlysis of the energy spectral show that if we were interested in the basis kinetic energy of the motions, then clearly it would be possible in many cases to limit ourselves to $L \approx 40$. However, here the meridional motion, whose basic scale close to the equator is much less than the scale of the azimuthal motions, would be greatly distorted.

3. THE HYDRODYNAMIC INTERPRETATION OF THE RESULTS OBTAINED. COMPARISON WITH EXPERIMENT

The numerical solutions of the problem posed in the thick annulus with $\delta = 1.33$ and $\varepsilon = -1$ have demonstrated the uniqueness of the solution of the axisymmetric current in the interval of Re considered.

The conformity with experimental and numerical results previously obtained [1 - 3, 8 - 10], the meridional current is concentrated in the lower latitudes (Figure 1) as Re increases, in the profile of the angular velocity there appears a point of inflection, and the spectrum of the kinetic energy shows that the basic part of the energy is contained in the large-scale motions. /21

The graph of the torque M as a function of Re (Figure 2) has no breaks up to the value of $Re \approx 410$, but near $Re \approx 54$ there is a point of inflection. Up to Re = 130, the experimental and numerical values of M agree with very good accuracy within 0.5%. For Re = 150, 200, and 250, the calculated values of M are given by circles in Figure 2; as is clear from the figure, the difference between the measurements and the calculated values is on the order of 2.5%, recorded when Re = 250, and it is possible in this connection that for this value of Re the accuracy of the current calculations declines for L = 31. Analysis of the spectra of the kinetic energy near the breaks noted by Munson [4] for Re_{c_1} and Re_{c_2} also discloses the absence of any reorganization in the current.

The results discussed together with the results of experiment [3, 11] make it possible to state a conclusion concerning the stability of a Couette spherical current in thick annulii in the interval for Re which was considered.

In the thin annulus with $\delta = 0.11$ and $\varepsilon = -1$, the basic axisymmetric Couette current exists up to Re = 1300 according to the calculations, which is somewhat larger than the first experimental value of the critical number Re = 1212 ± 25. For values of Re > 1260, only a special type of disturbance makes is possible to obtain numerically a current regime with two annular vortices. This impossibility of obtaining regime 1 from the basic current by a simple increase in Re is connected, obviously, with the condition of symmetry of the current relative to the equator which we imposed. In an experiment [6], the appearance of regime 1 was connected with the momentary disruption of such symmetry at the limit of stability. /22

The cause of the approximately 4% divergence in the numerical and experimental values of the first critical value of Re (Re_c = 1260 by calculation; Re_c = 1212 ± 25 by experiment) is still not clear to us.

Just as in the case of experiment, calculations show that for supercritical values of Re there exist several different steady-state current regimes at one and the same point in space. On the diagram (Figure 4a), the regions of existence (relative to Re) corresponding to the regimes of the calculations are denoted by lines opposite the numerals 0, 1, 2, 3, and 4. The arrows indicate the transition from one regime to another as Re increases without the introduction of additional disturbances; a dotted arrow denotes the passage from the basic current to regime 1 when disturbances of special type are introduced into the current. The upper mark corresponds to the domain of existence of these regimes in the experiment [6]. The wavy form of the mark indicates the appearance of sinusoidal disturbances in the annular vortices in the corresponding regimes.

Regimes 3 and 4, as is clear from the diagram, exist for larger values of Re than in the experiment. Regime 4 for Re - 2150 and regime 3 for Re = 2300 are reorganized into essentially non-axisymmetric regimes with spirals [5, 6]. In the calculations, both solutions for Re = 2700 become oscillations with a period approximately equal to the period of one revolution. For the present, it is difficult to say whether these oscillations are purely a calculational phenomenon, or the period axisymmetric regimes are solutions of the Navier-Stokes equations. If the latter is true, then they must be unstable relative to the non-axisymmetric disturbances, since in the experiment on spherical [6] and cylindrical [17] annulii no periodic axisymmetric current was observed.

Qualitatively, the forms of the currents for the regimes obtained by calculation and by experiment compare favorably also. /23 Thus in regime 4, the third annular vortex from the equator always occupies more space than the remaining vortices, in the experiment as well as in the calculations. Supercompression of the lines of flow and the formation of closed vortices in the basic current (current of the "cat's eyes" type), obtained in the numerical calculation (Figures 7, 8, 9, 20B) were recorded in experiment [6] in the form of regions with large velocity gradients (the broad, dark belts below the annular vortices in Figure 20a).

CONCLUSIONS AND SUMMARY

The results of the numerical investigation of nonlinear steady-state axisymmetric currents in a viscous incompressible liquid in a thick (δ = 1.33) and a thin (δ = 0.11) annulus when only the internal sphere rotates (ε = -1) in the indicated invervals of variation of Re make it possible to draw the following conclusions:

1. In the interval 5 $\leq$ Re $\leq$ 250 in a thick annulus, there was obtained (in agreement with experiment) a unique steady-state axisymmetric solution — the basic Couette spherical current.

2. The absence of breaks in the curves of the torques M(Re) (Figure 2) and the kinetic energy E(Re) (Figure 3), and also the absence of qualitative changes in the spectrum for the kinetic energy of the current as Re increases, make it possible to draw an inference concerning the stability of the Couette spherical current in a thick annulus relative to the steady-state axisymmetric disturbances in the Re interval considered. Taking into account the results of experiment [11], this conclusion can be generalized to the stability of the Couette spherical current in thick annuli relative to arbitrary disturbances when Re $\leq$ 410.

3. In a thin annulus, only those steady-state axisymmetric current regimes are obtained numerically which were observed experimentall, i.e., the basic current and currents with two, four, six, /24
and eight annular vortices. The regions of existence of the numerical solutions, as is clear from Figure 4, can be distinguished from the regions obtained experimentally. The prolongation of certain current regimes into the region of larger Re values can be explained by the fact that the conditions of axisymmetry and symmetry relative to the equator are imposed on the motions, and the current regimes observed in these regions are essentially non-axisymmetric and non-symmetric with respect to the equator.

4. The basic steady-state axisymmetric Couette current in a thin annulus exists up to the value Re = 1300, which is somewhat larger than the experimental value of the first critical Reynolds number Re = 1212 $\pm$ 25, above which the basic current turns out to be unstable.

5. In the supercritical region, the numerical as well as the physical experiment gives a non-unique solution for the same Re values.

6. In a thin annulus, the spectral characteristics of the velocity components disclose the following features of the secondary currents: a large part of the energy of differential rotation during supercritical regimes is contained in maximum scale motions

(the wave numbers $\ell \approx 2 - 4$), and the energy of the meridional motions have two approximately equivalued maxima for $\ell \approx 2$ and $\ell \approx 40$, i.e., large-scale and small-scale motions which are equally justified from the standpoint of energy. It is interesting to note that as Re increases within the very same regime, the predominant scale of the small-scale part of the periodic motions increases, i.e., the wave number ℓ decreases.

Thus, numerical modeling of the nonlinear Couette spherical current and the secondary currents which emerge for the supercritical values of Re produced results which are in good agreement with experiment. As a supplement to a physical experiment, the calculations make it possible to determine the total kinetic energy of currents, its spectral distribution, to study the fine structure of currents, and in disputed cases to resolve the question of the stability of currents. /25

APPENDIX

In the calculations, the time-related quantities for the $(n + 1)^{st}$ annulus were obtained after completion of the calculations for the n^{th} annulus. At this time there were files for the quantities $U_\ell^n(k), V_\ell^n(k), W_\ell^n(k)$ in the storage of the computer by means of which, with the aid of formula (2.3), the values

$u_r^n(k,\theta_j), \frac{\partial u_r^n(k,\theta_j)}{\partial \theta}, u_\theta^n(k,\theta_j)$, etc., were calculated. By means of these quantities, the nonlinear terms $\mathcal{F}_i^n(k,\theta_j,t)$, $i = 1, 2, 3$ were computed. To reduce the time to calculation $\mathcal{F}_i^n$, at the beginning before undertaking the problem, three matrices were calculated and the results stored in the memory of the computer. The elements $a_{j\ell}$ of these matrices are (in the generally accepted notation):

$$\mathcal{P}_e^0(\cos\theta_j),\ l=0,2,\ldots,L-1;\quad j=0,1,\ldots,\frac{L-1}{2};$$

$$\mathcal{P}_e^1(\cos\theta_j),\ l=2,\ldots,L-1;\ j=1,\ldots,\frac{L-1}{2}; \qquad (A.1)$$

$$\mathcal{P}_e^1(\cos\theta_j),\ l=1,\ldots,L-2;\ j=1,\ldots,\frac{L-1}{2}.$$

To calculate the values of $\Phi_{i,e}^{n}(k)$, (with respect to $\mathcal{F}_i^{n}(k,\theta_j)$) the inverse f the matrices (a.1) were stored in the computer.

After calculating the values of $\Phi_{i,e}^{n}(k)$, the difference equations (2.8) and (2.9) were solved. Here, U_e, V_e, P_e are found from equations 1, 2 and 4 with the help of a matrix trial run, and W_e is obtained with the aid of the usual run. (We draw attention to the fact that no difficulties are encountered here because of the absence of boundary conditions for ρ.) /26

The major part of machine time was spent in calculating $\mathcal{F}_i$ and $\Phi_{i,e}$.

Choice of the function f is quite arbitrary. We assume:

$$f = r^3 + b r^2 + c r + d$$

$$b = -1.5\,(2+\delta)$$

$$c = \delta + b^2/3\ ;\ d = -(b + c)$$

The computed points $r(k)$ on the boundaries $r = 1$ and $r = 1+\delta$ were thicker here than in the center of the annulus. In calculations relative to $\delta = 1.33$, the number of points along the radius $K = 20$, and in calculations for $\delta = 0.11$, we assumed $K = 10$.

The calculations for $\delta = 1.33$ were carried out with the values of the calculated parameter $\tau = 0.6$; when $\delta = 0.11$, it was assumed that $\tau = 0.2$.

The time to determine the solution depended on the initial data and the value of Re. Here near the critical values of Re, at which the current of the given regime lost stability, the time to obtain the solution increased. Thus, e.g., when Re = 1750 with initial values corresponding to Re = 1800, the fourth sign for torque M was determined after 400 steps with respect to t, and for Re = 1700 and initial values corresponding to Re = 1750, 1200 steps were required.

Since we are interested in cases in which the solution of the steady-state equations is not unique, we devoted special attention to the extent to which these equations are effectively satisfied. Let us consider the following figures: when Re = 1250 in the first of the equations, $\frac{\partial \omega_z}{\partial t} = -0{,}11175871 \times 10^{-6}$; here the contribution of /27 the energy terms = 0.90864956; that of the viscosity terms = -0.0046423005, and of the pressure gradient = -0.086222768.

The processing and development of the results were carried out according to separate programs. Since the solutions are presented in the form of interpolational sums, we were able to calculate the values of the desired functions at any point θ, which made it possible to obtain a detailed picture of the current in the equatorial region (Figure 7 - 9).

REFERENCES

1. Khlebutin, B. H. The Stability of the Motion of a Liquid between Rotating and Fixed Concentric Spheres. MZHG, No. 6, 1968. /28

2. Sawatzki, V. O. and J. Zierep.

   Acta Mech., Vol. 9, No. 1, 1970.

3. Yavorskaya, I. M., Yu. N. Belyayev and A. A. Monakhov. An Experimental Study of the Couette Spherical Current. DAN SSSR, Vol. 221, No. 5, 1975.

4. Munson, B. R. and M. Menguturk. Viscous Incompressible Flow Between Concentric Rotating Spheres. J. Fl. Mech., Vol. 69, No. 4, 1975.

5. Yavorkaya, I. M., Yu. N. Belyayev and A. A. Monakhov. A Study of Stability and Secondary Currents in Rotating Spherical Annulii for Arbitrary Rossby Numbers. DAN SSSR, Vol. 237, No. 4, 1977.

6. Petrov, G. I., I. M. Yavorskaya, Yu. N. Belyayev, et al. Modeling Dynamic Processes in the Atmospheres of Planets. Preprint IKI, No. 255, 1975.

7. Pearson, C. A. A Numerical Study of the Time-Dependent Viscous Flow Between Two Rotating Spheres. J. Fl. Mech., Vol. 28, No. 2, 1967.

8. Yakushin, V.I. On the Steady-State Motion of a Viscous Liquid in a Spherical Annulus. MZHG, No. 6, 1968.

9. Astaf'yeva, N. M., I. Yu. Brailovskaya and I. M. Yavorskaya. On the Motions of a Viscous Compressible Heat-Conducting Liquid in a Spherical Annulus. Preprint IKI AN SSSR No. 96, Dep. No. 5050-72/

10. Munson, B. R. and D. D. Joseph. Viscous Incompressible Flow Between Concentric Rotating Spheres, Parts 1, 2. J. F. Mech, Vol. 49, No. 2, 1971.

11. Belyayev, Yu. N., A. A. Monakhov and I. M. Yavorskaya. The Stability of the Couette Spherical Current in Thick Annulii During Rotation of the Internal Sphere. MZHG, No. 2 (in press), 1978. /29

12. Yavorskaya, I. M. and N. M. Astaf'yeva. Currents of a Viscous Liquid in Spherical Annulii. Preprint IKI AN SSSR, Ob-10, 1974.

* Translators Note: MzhG = Izvestiya Akademii Nauk SSSR, Meknanika Zhidkosti i Gaza

13. Yakushin, V. I. On the Stability of the Motion of a Liquid in a Spherical Annulus. Uch. zap. PGU, No. 248, 1971, Part 3.

14. Bonnet, J. P. and T. Alziary de Roquefort. Flow between Two Rotating Concentric Spheres. J. de Mec., Vol. 15, No. 3, 1976.

15. Wimmer, M. Experiments on a Viscous Flow between Concentric Rotating Spheres. J. Fl. Mech., Vol. 78, No. 2, 1976.

16. Babenko, K. I., N. D. Vvedenskaya and M. G. Orlova. Calculation of the Steady-State Streamline Flow of a Viscous Liquid around a Circular Cylinder. ZH. vych. mat. i mat. fiz., Vol. 15, No. 1, 1975.

17. Coles, D. Transition in Circular Couette Flow. J. Fl. Mech., Vol. 21, No. 3, 1965.

CAPTIONS TO THE FIGURES

Figure 1. Flow functions of the meridional current and the lines of constant angular velocity in the annulus $\delta = 1.33$, Re = 200 /30

Figure 2. The curve of the torque $\hat{M}(Re)$ for the annulus $\delta = 1.33$. Experiment and theory $\hat{M} = M_0 / \frac{7}{3} \pi r_2^3 \Omega_1 \mu$.

Figure 3. The curve of the kinetic energy $E(Re)$ for the annulus $\delta = 1.33$

Figure 4. Existence diagram for various regimes of currents (a) and the wave length of a vortex near the equator as a function of the number Re (B) in the thin annulus $\delta = 0.11$

Figure 5. The spectrum $U_\ell(\ell)$ for various L when Re = 1300 in the annulus $\delta = 0.11$

Figure 6. The spectrum $U_\ell(\ell)$ for various L when Re = 1500 in the annulus $\delta = 0.11$

Figure 7. The current functions $\psi \cdot 10^2$ and the lines of constant angular velocity in the annulus $\delta = 0.11$

a) Re = 1600 regime 2,
b) Re = 1600 regime 3,
c) Re - 1270 regime 1

Figure 8. The same as Figure 7 with Re = 1900

a) regime 2,
b) regime 3,
c) regime 4

Figure 9. The same as Figure 7 with Re = 2200

a) regime 2,
b) regime 3,
c) regime 4

Figure 10. The current function and the angular velocity as functions of θ when $r = 1.049$, and the spectra of $U_\ell(\ell)$ and $W_\ell(\ell)$ for the basic current when Re = 1270

Figure 11. Ditto for regime 1 when Re = 1270 /31

Figure 12. Ditto for regime 2 when Re = 1600

Figure 13. Ditto for regime 3 when Re = 1600

Figure 14. Ditto for regime 2 when Re = 1900

Figure 15. Ditto for regime 3 when Re = 1900

Figure 16. Ditto for regime 4 when Re = 1900

Figure 17. Ditto for regime 2 when Re = 2200

Figure 18. Ditto for regime 3 when Re = 2200

Figure 19. Ditto for regime 4 when Re = 2200

Figure 20. The stream lines $\psi \cdot 10^2$ and a photograph of the current of region 4 when Re = 1900 and $\delta = 0.11$

Figure 21. The spectra of the kinetic energy of the currents in the thin annulus $\delta = 0.11$

Figure 22.
a) Re = 1270 region 0
b) Re = 1270 regime 1
c) Re = 1600 regime 2
d) Re = 1600 regime 3

Figure 22. The same as Figure 21
a) Re = 1900 regime 2
b) Re = 1900 regime 3
c) Re = 1900 regime 4
d) Re = 2200 regime 2
e) Re = 2200 regime 3
f) Re = 2200 regime 4

Figure 23. The kinetic energy E and the torque M as functions of Re in the thin annulus δ=0.11

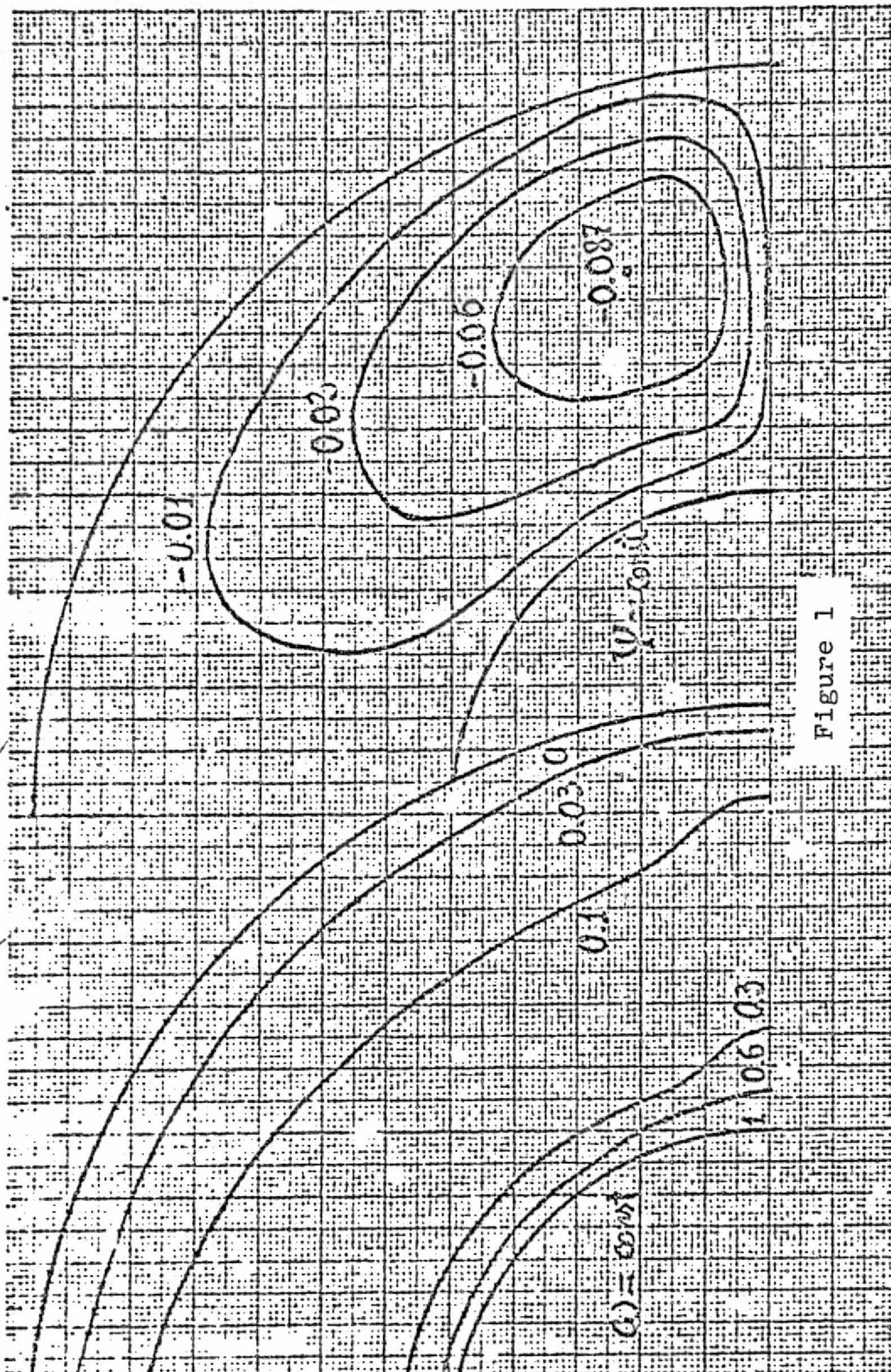

Figure 1

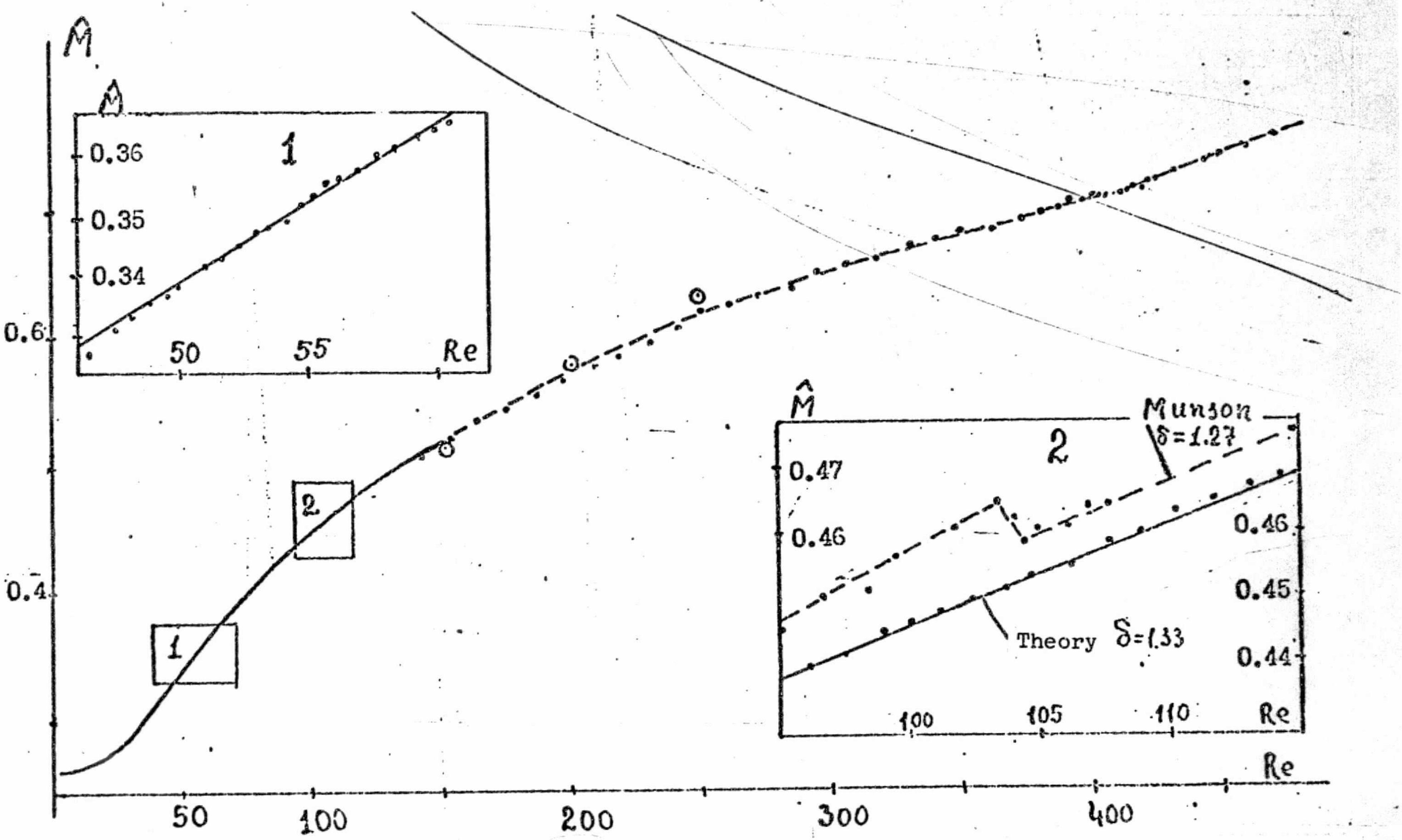
M̂
0.36
0.35
0.34
1
50
55
Re
0.6
0.4
2
Munson
δ=1.27
0.47
0.46
0.45
0.44
Theory δ=1.33
100
105
110
200
300
400

Figure 2

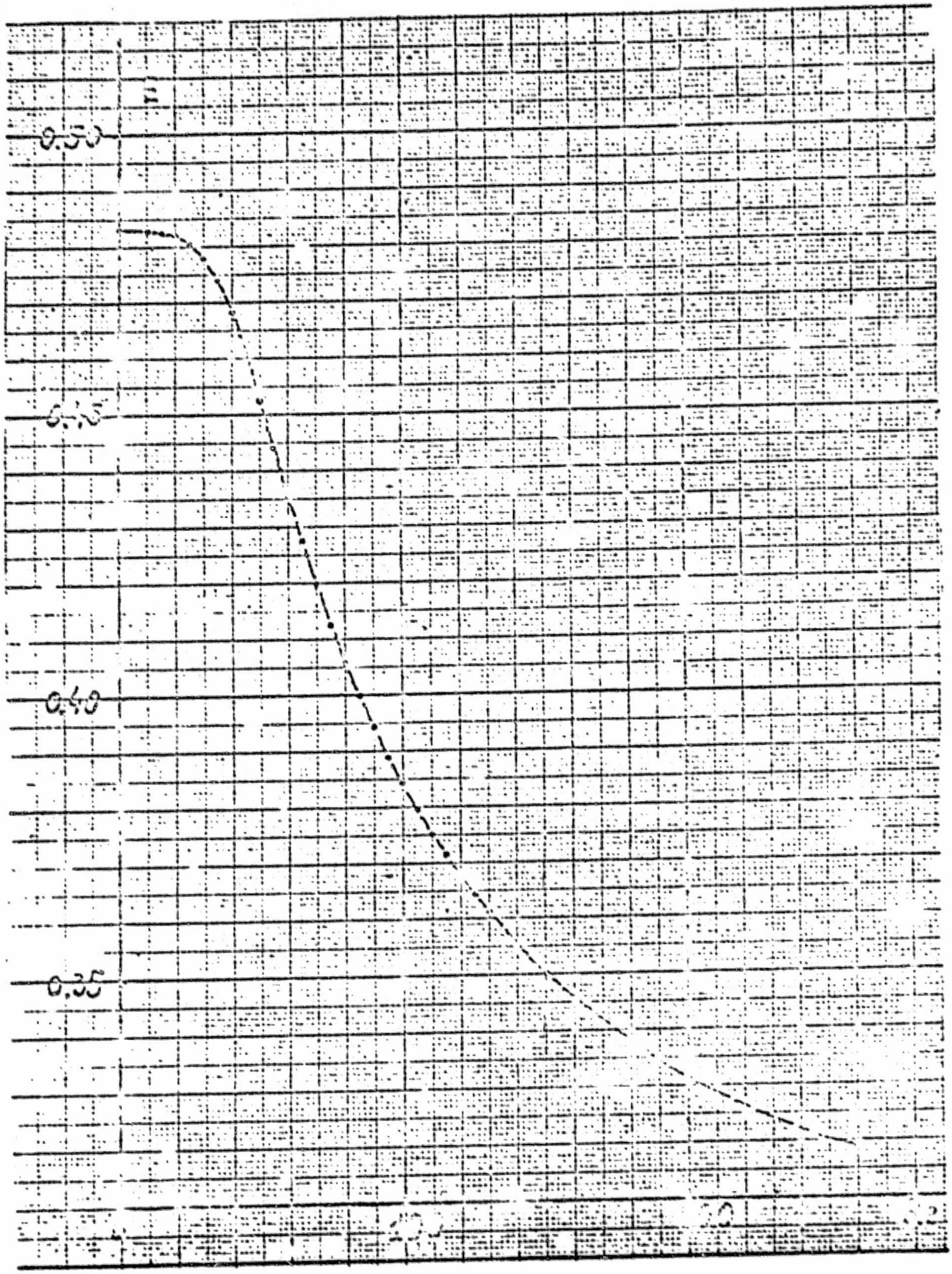

Figure 3

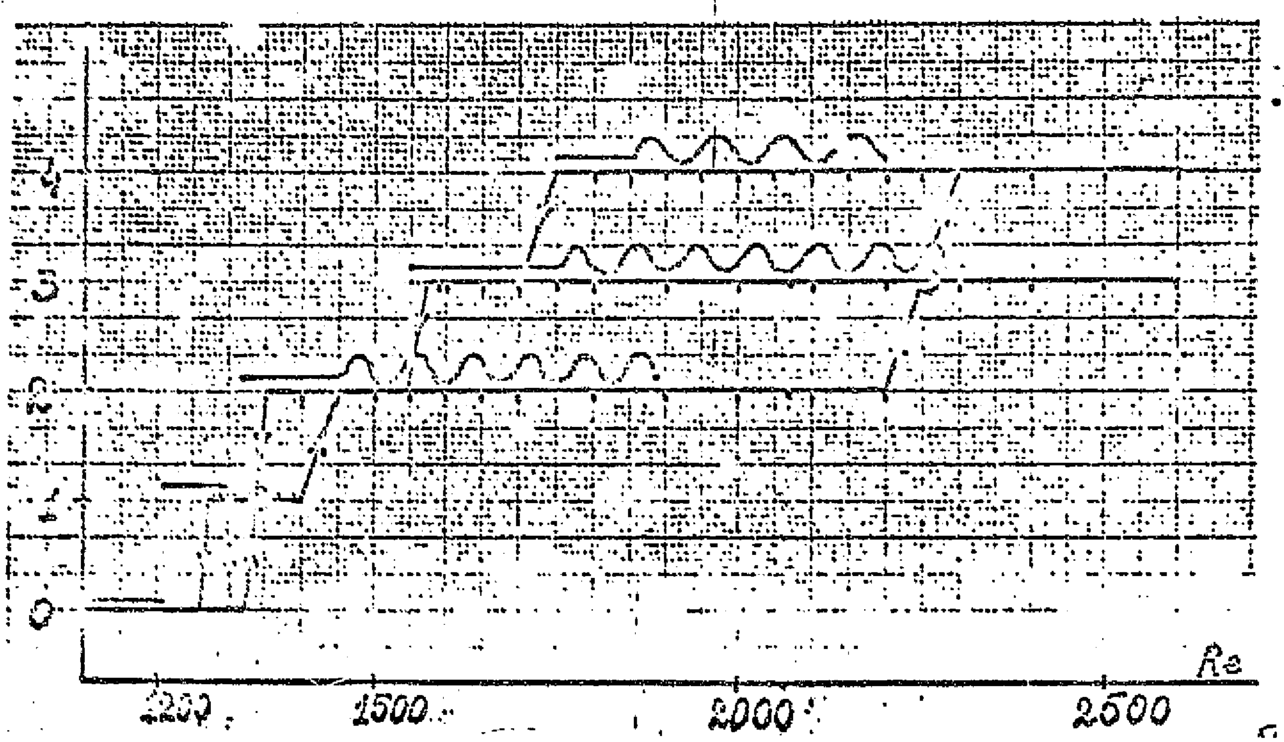

Figure 4a

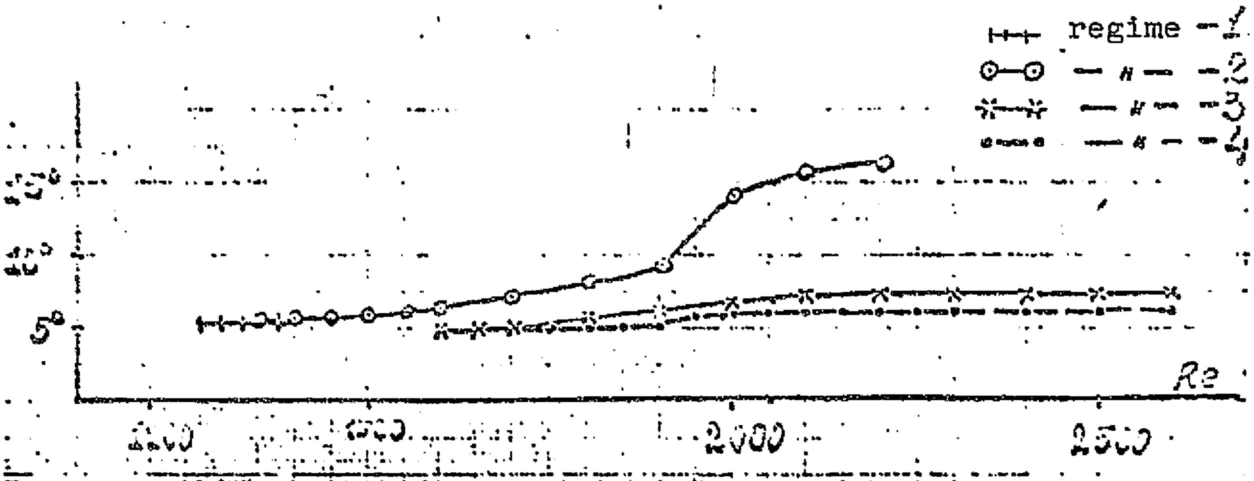

Figure 4b

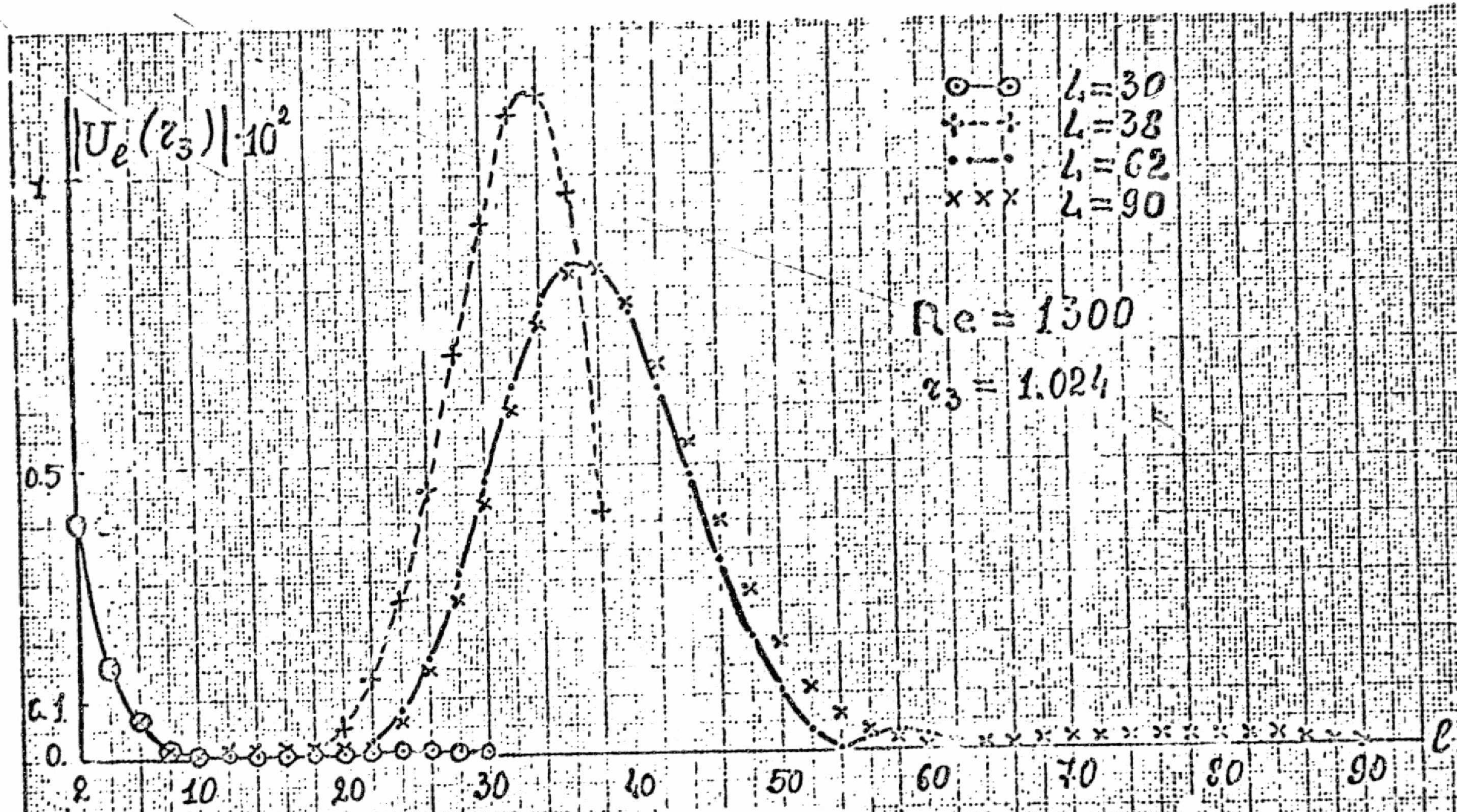

$|U_l(r_3)| \cdot 10^2$
L=30
L=38
L=62
L=90
Re = 1300
$r_3 = 1.024$
1
0.5
0.1
0.
2
10
20
30
40
50
60
70
80
90
l

Figure 5

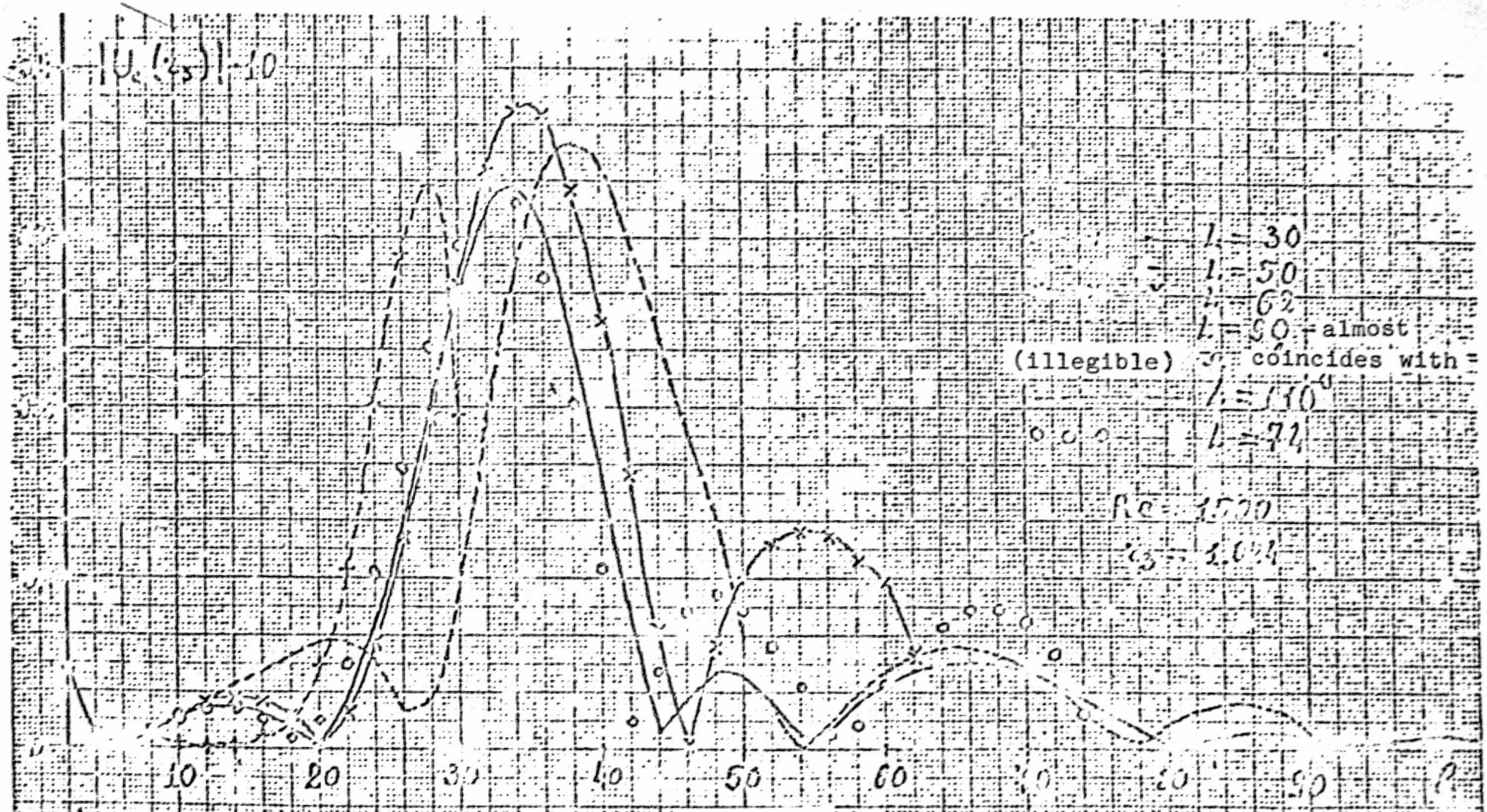
$|U_c(\eta_3)| \cdot 10$
$l = 30$
$l = 50$
$l = 62$
$l = 90$ almost
(illegible) coincides with
$l = 110$
$l = 71$
10
20
40
50
60

Figure 6

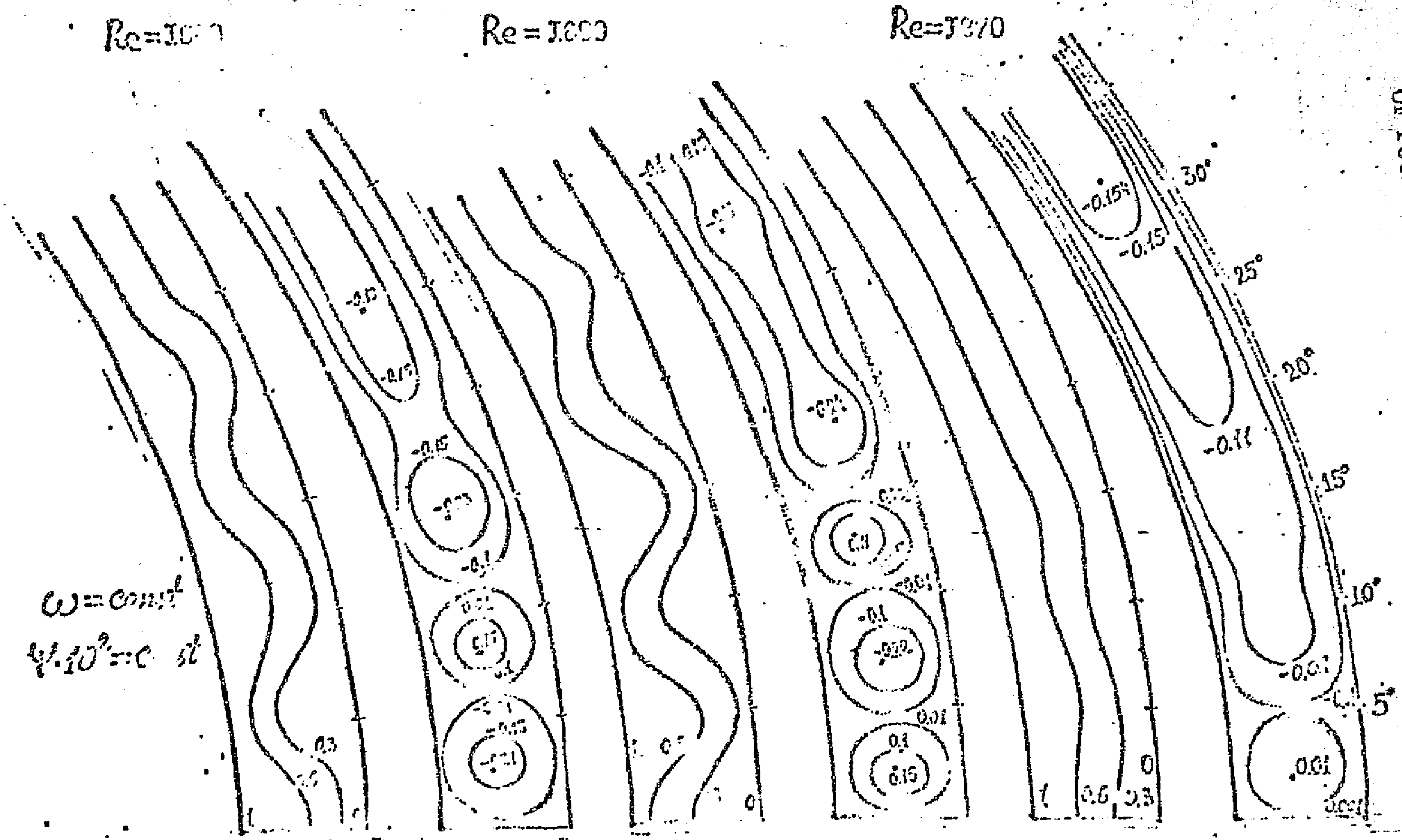

Figure 7a

Figure 7b

Figure 7c

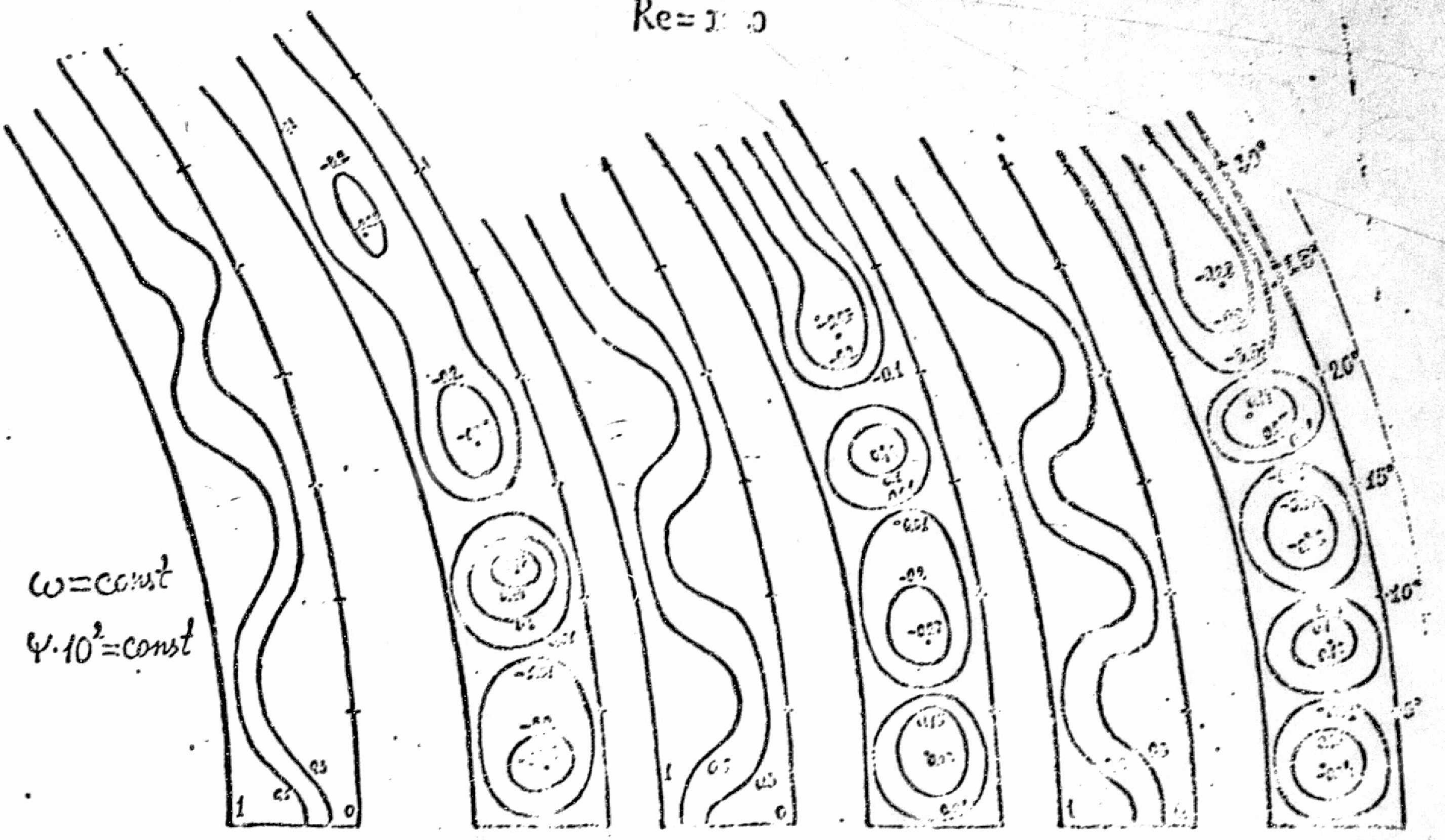

Figure 8a Figure 8b Figure 8c

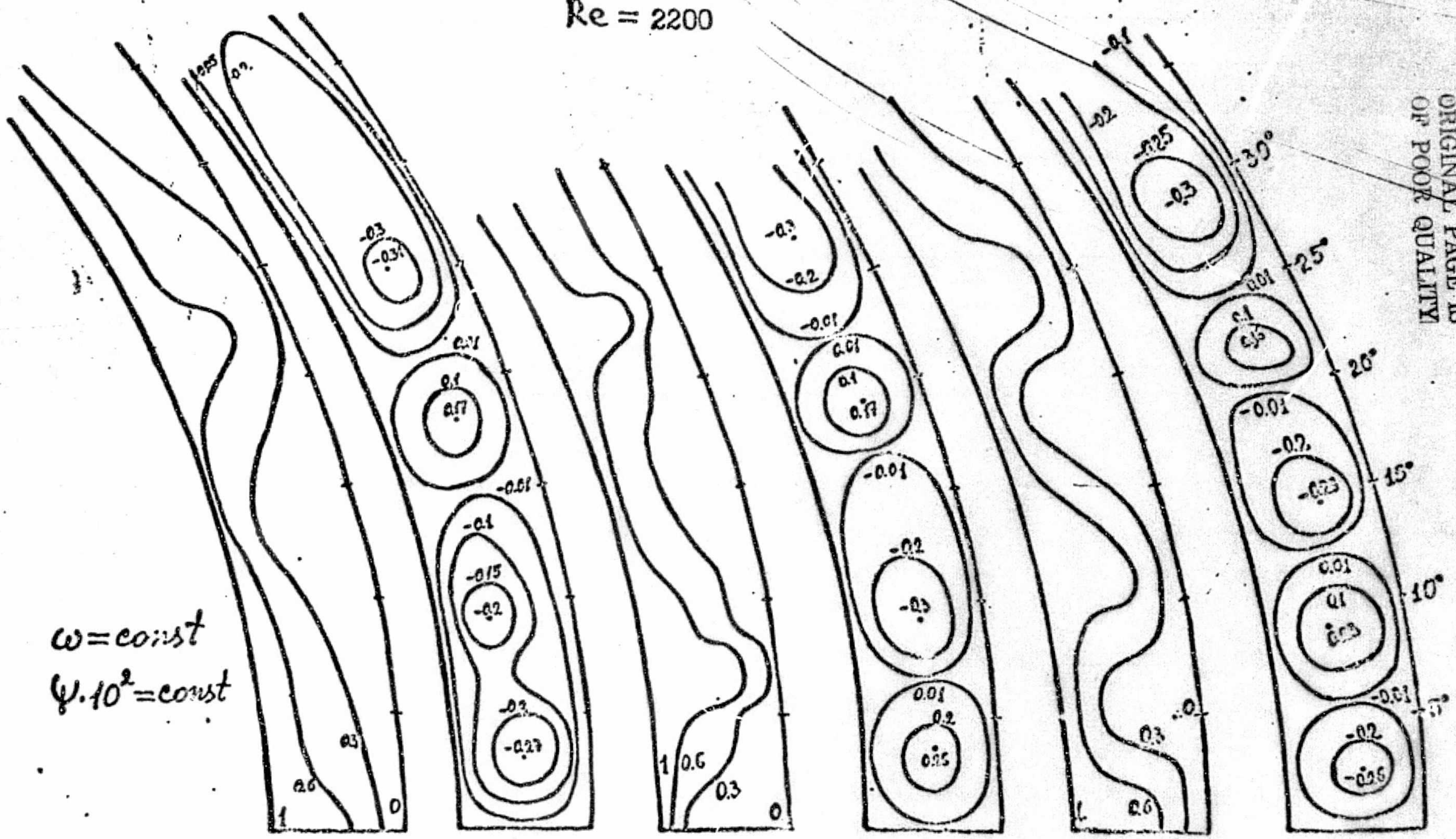

Figure 9a

Figure 9b

Figure 9c

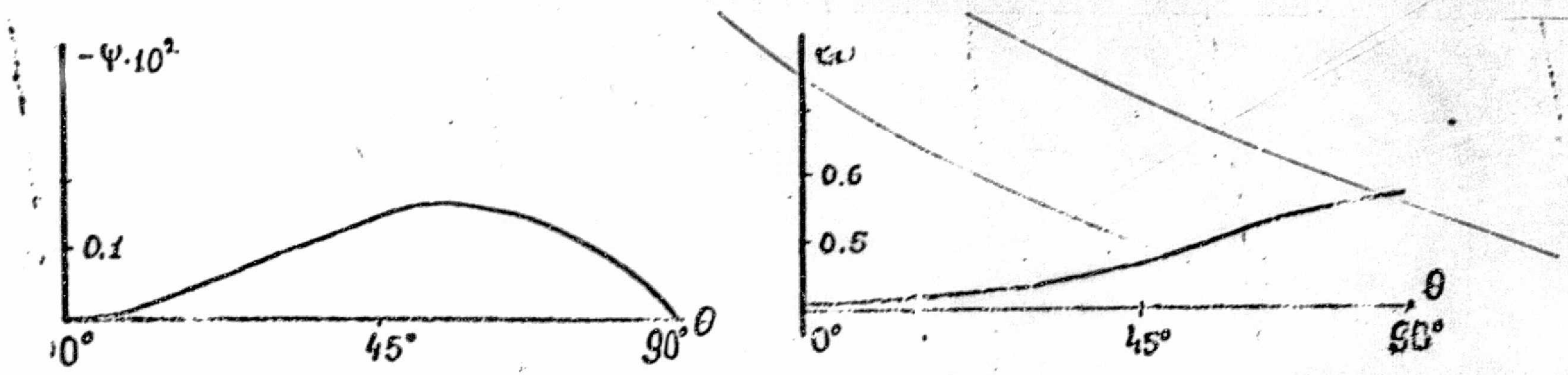

Re= 1270.

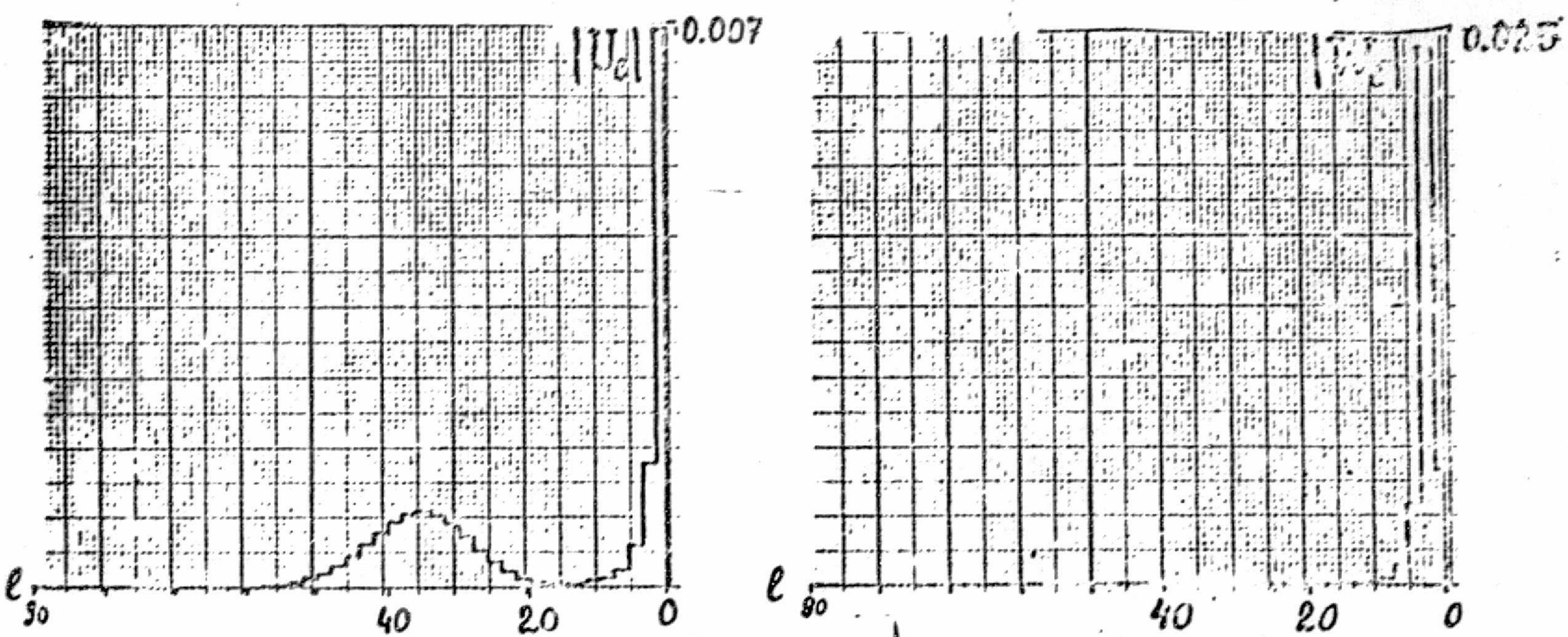

Figure 10

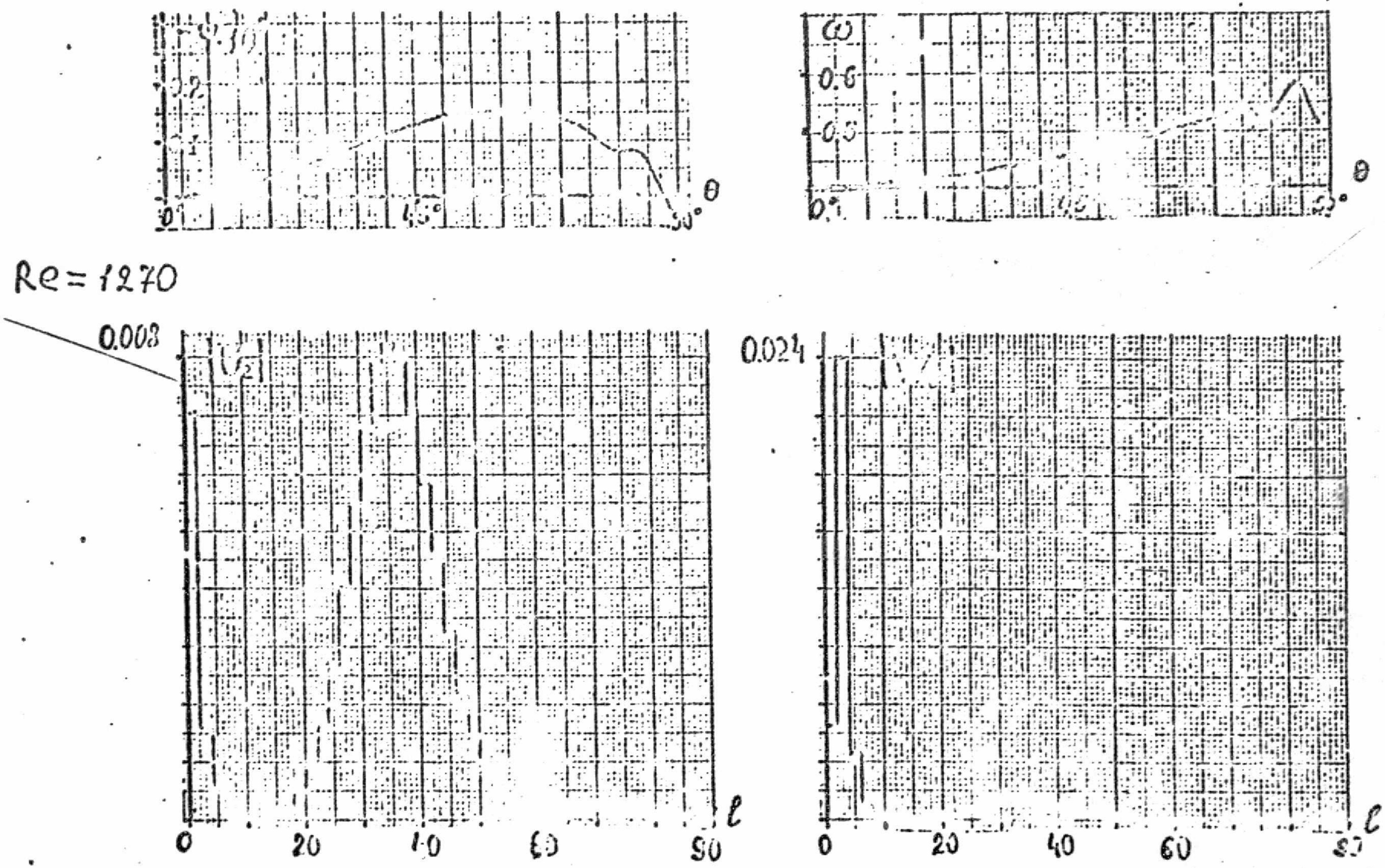

Figure 11

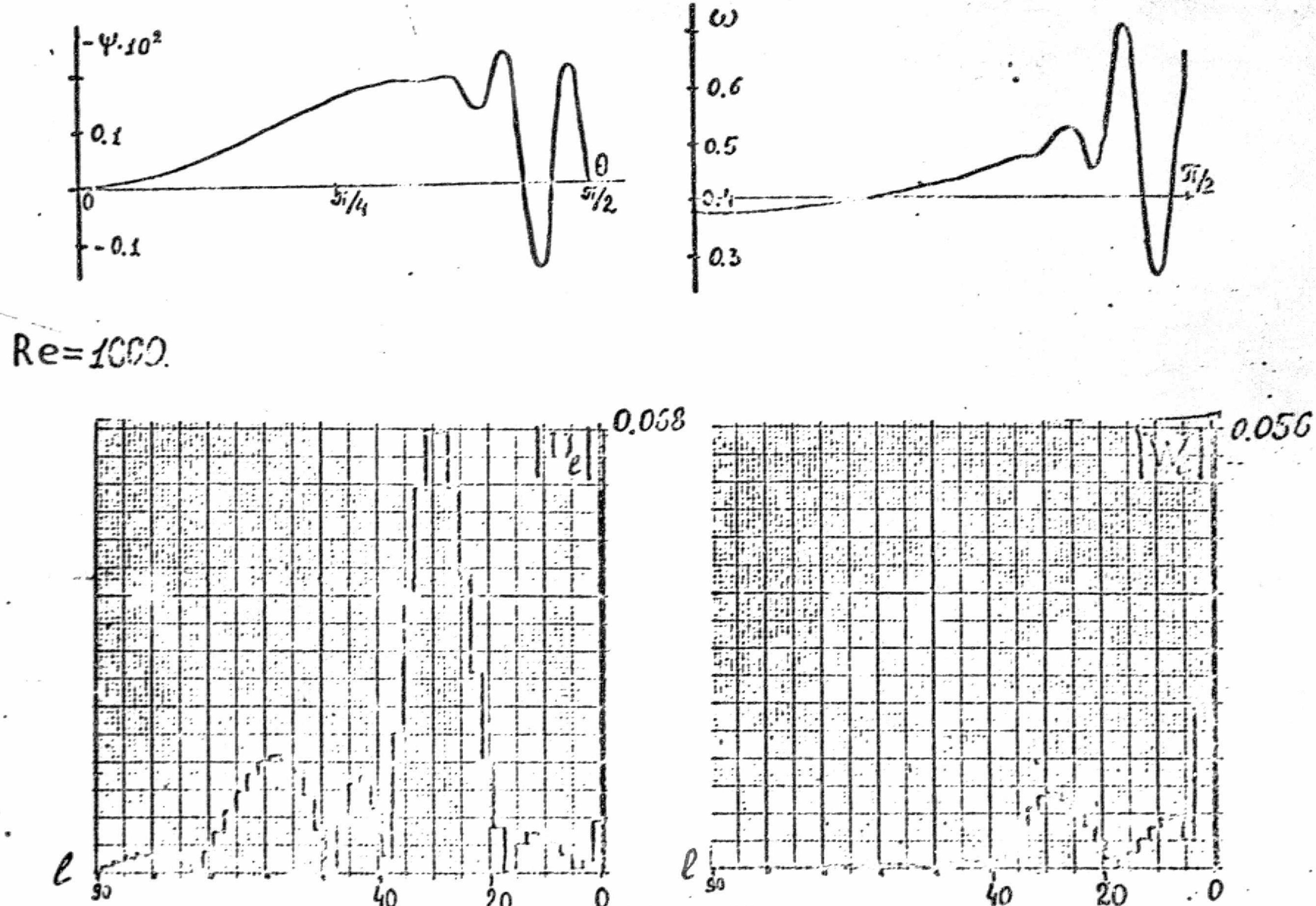

Figure 12

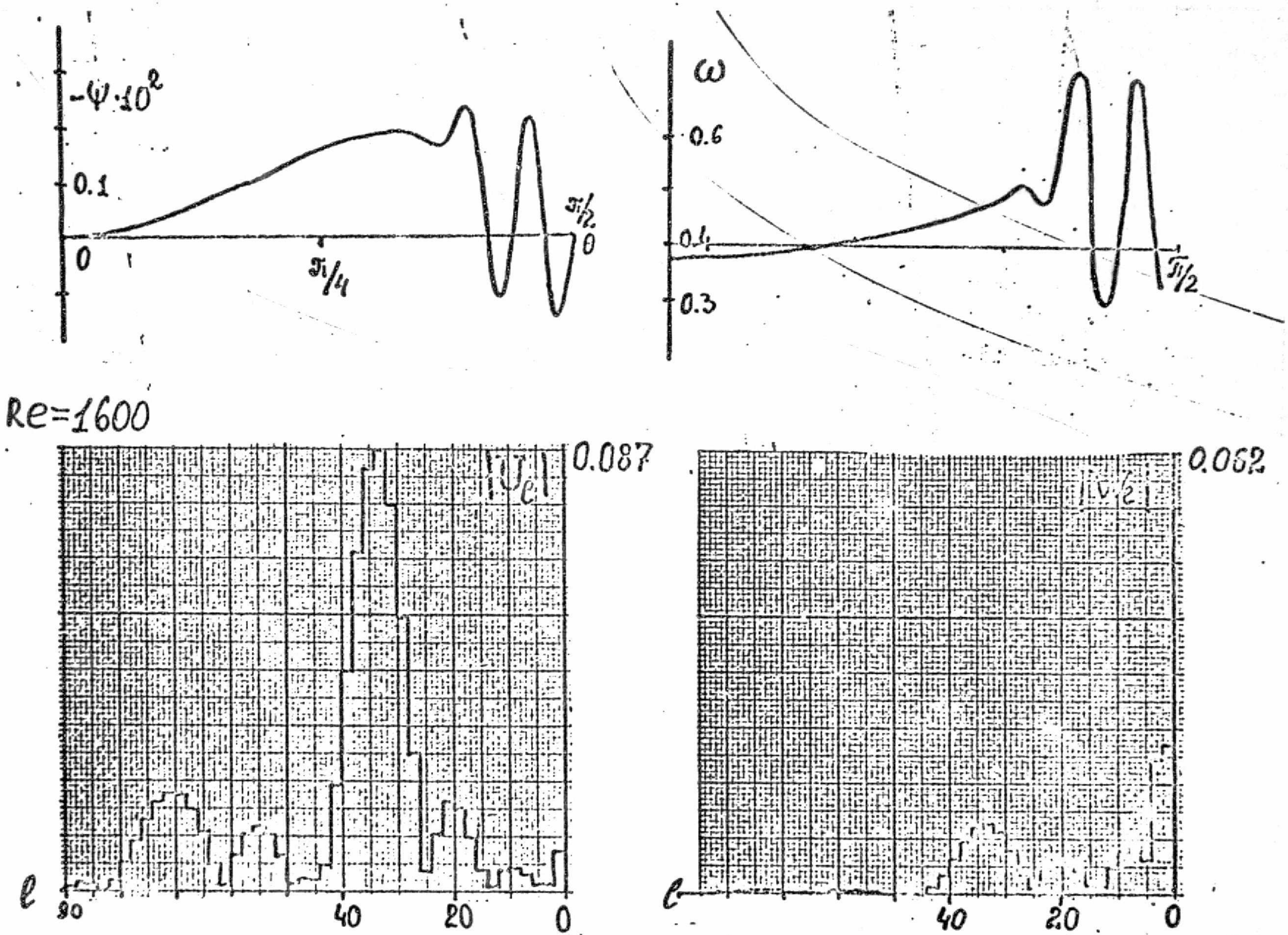

$-\psi \cdot 10^2$
0.1
0
$\pi/4$
$\pi/2$
θ
ω
0.6
0.1
0.3
$\pi/2$
Re=1600
0.087
$|U_\ell|$
ℓ
40
20
0
0.062
ℓ
40
20
0

Figure 13

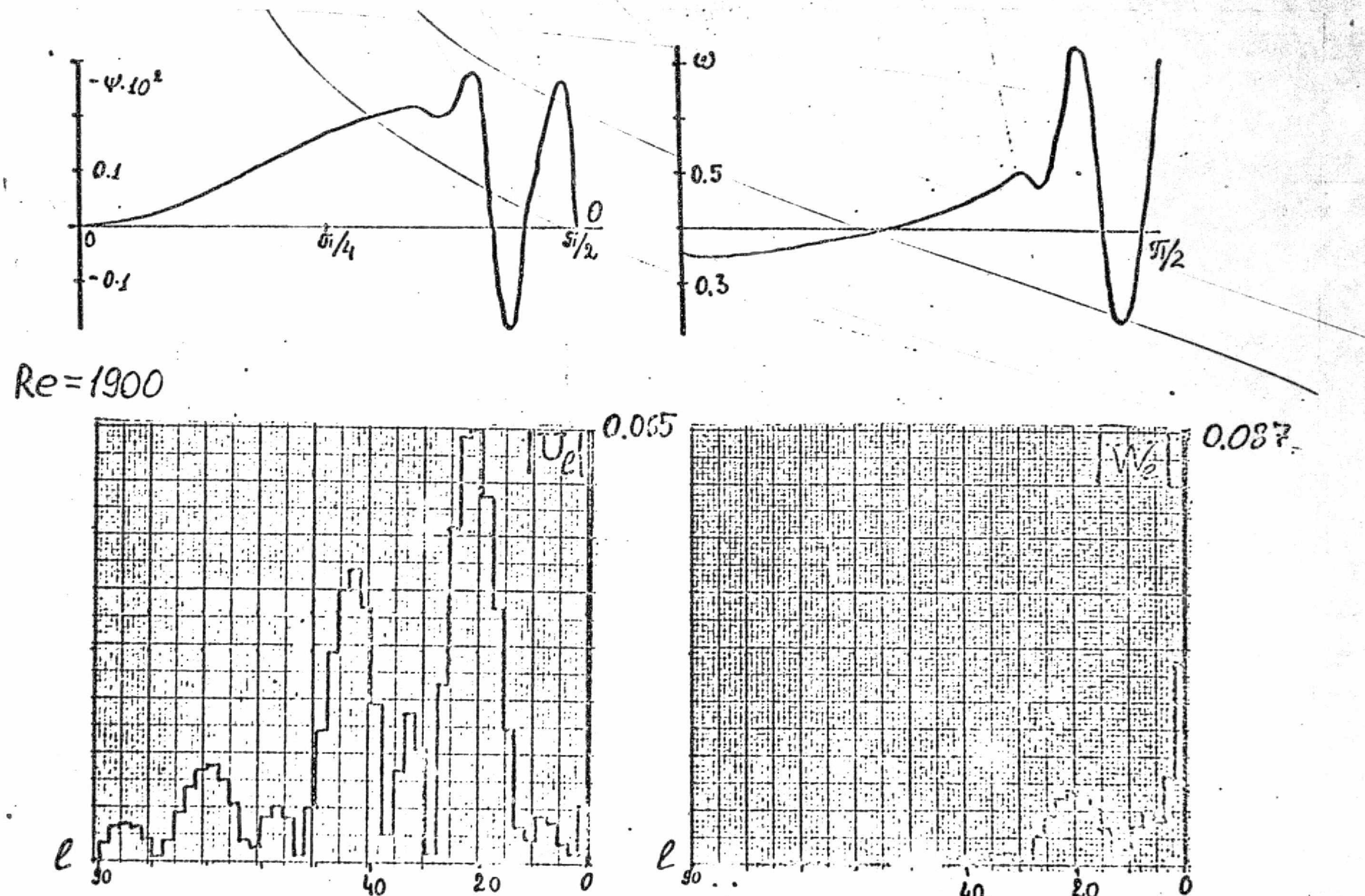

Figure 14

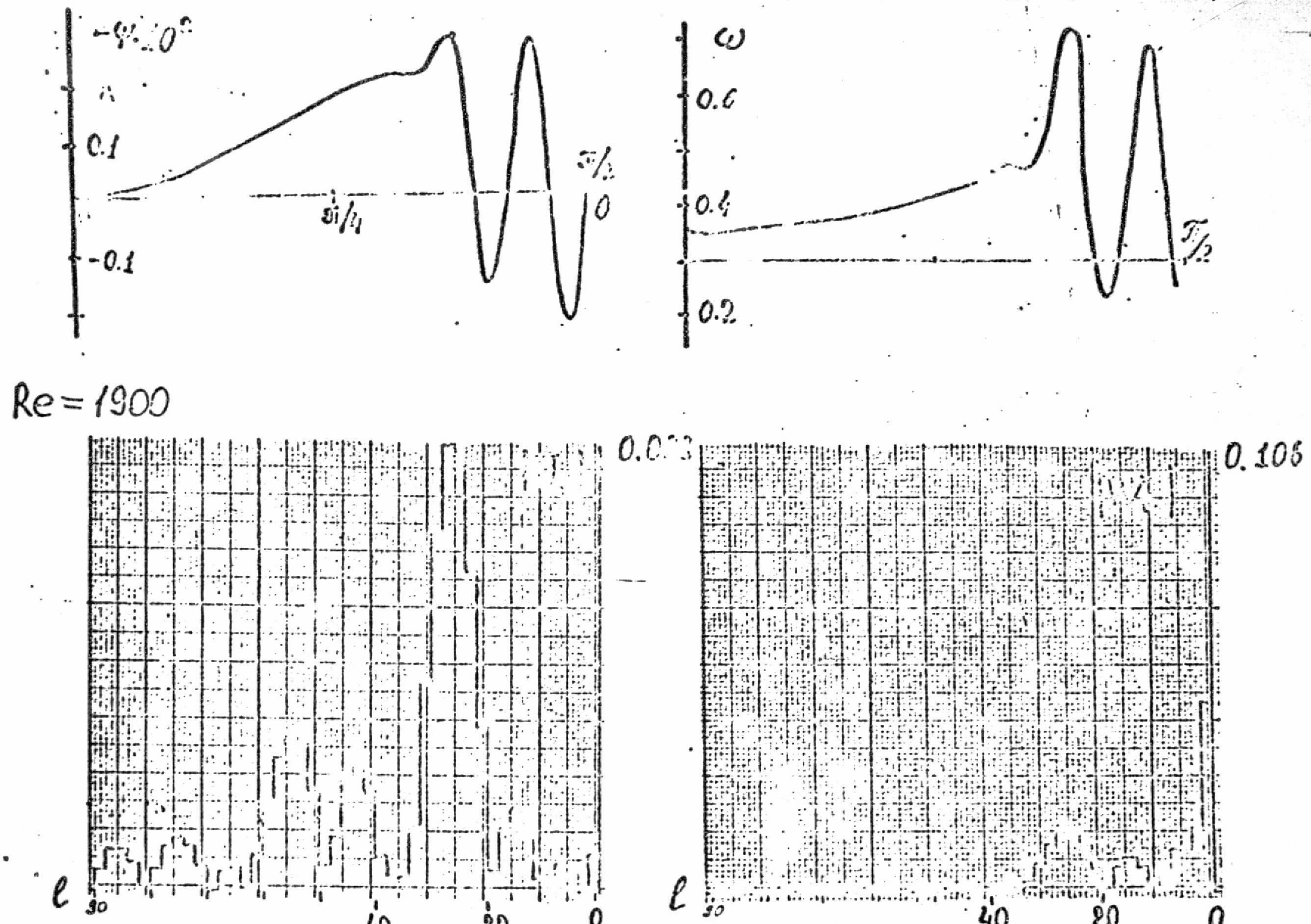

Figure 15

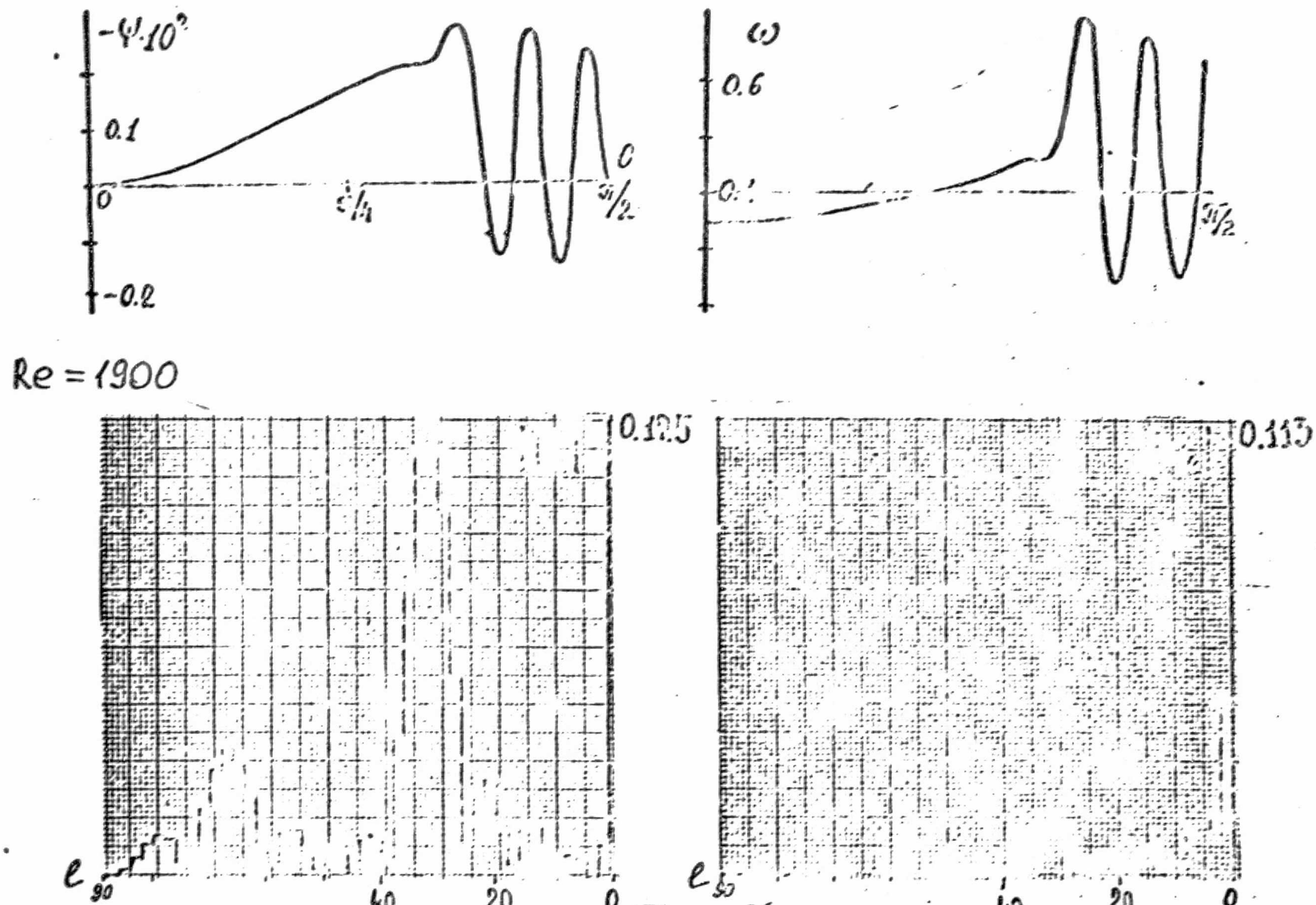

Figure 16

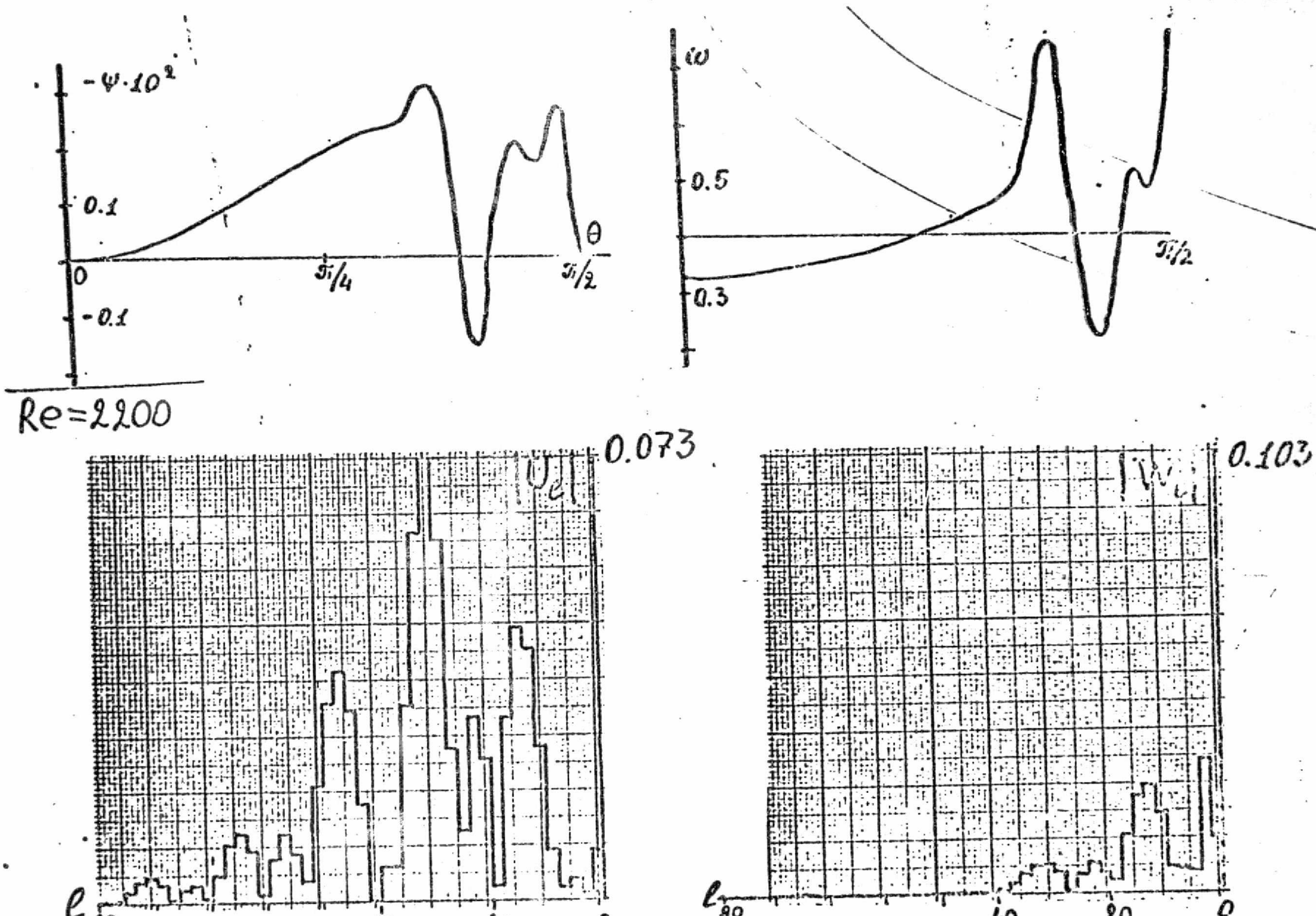

Figure 17

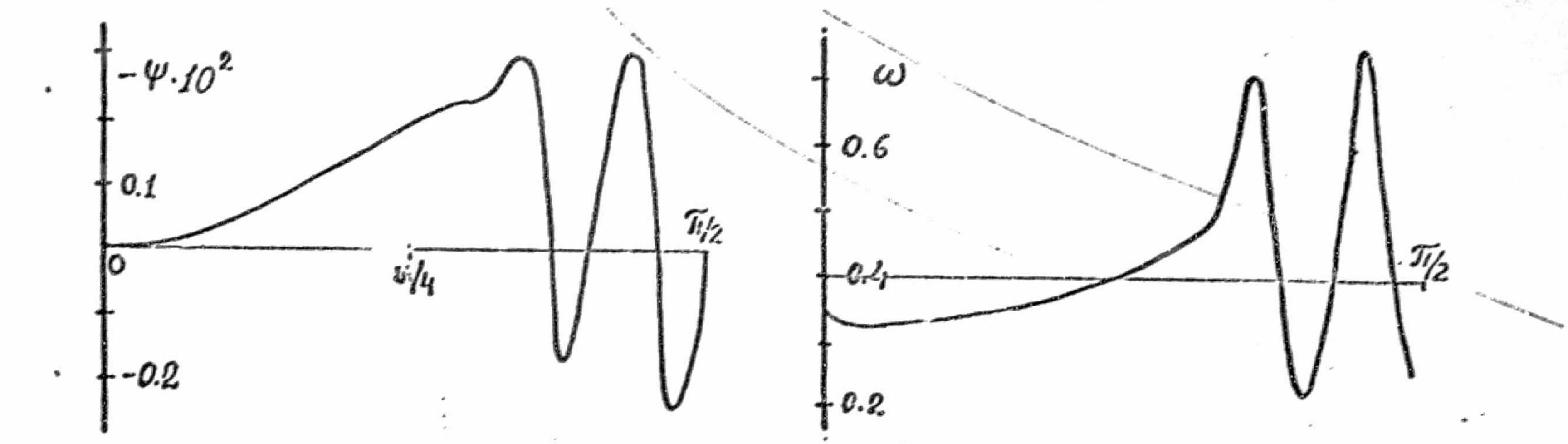

Re = 2200

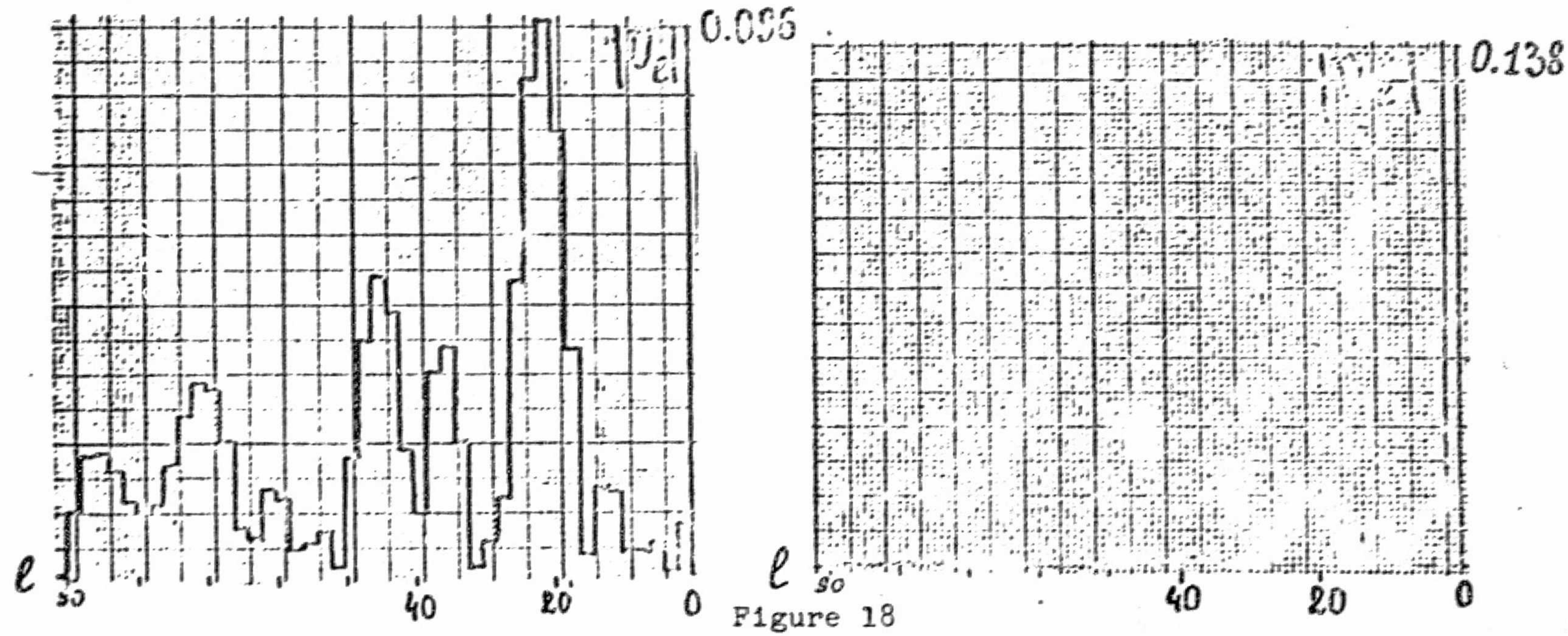

Figure 18

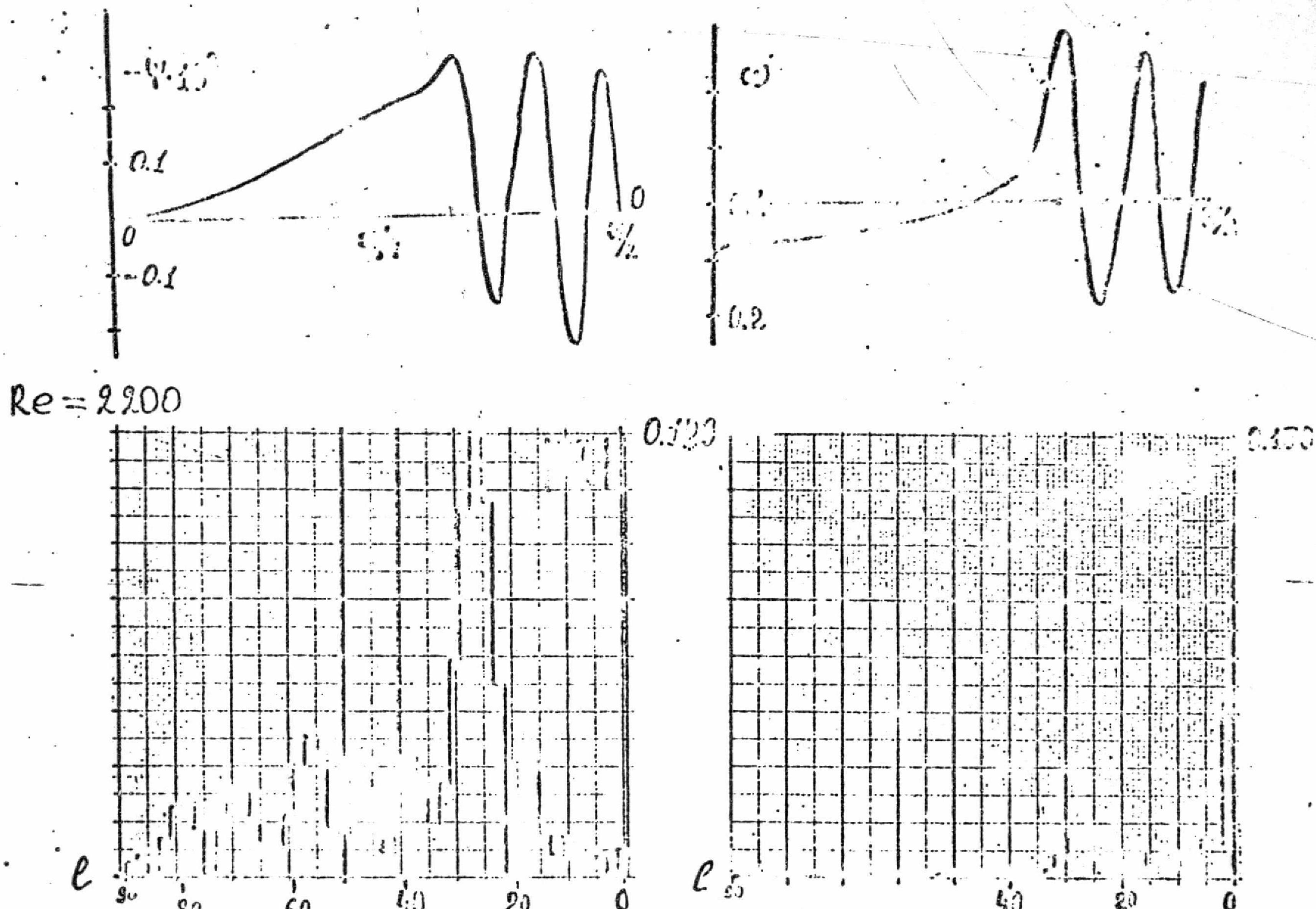

Figure 19

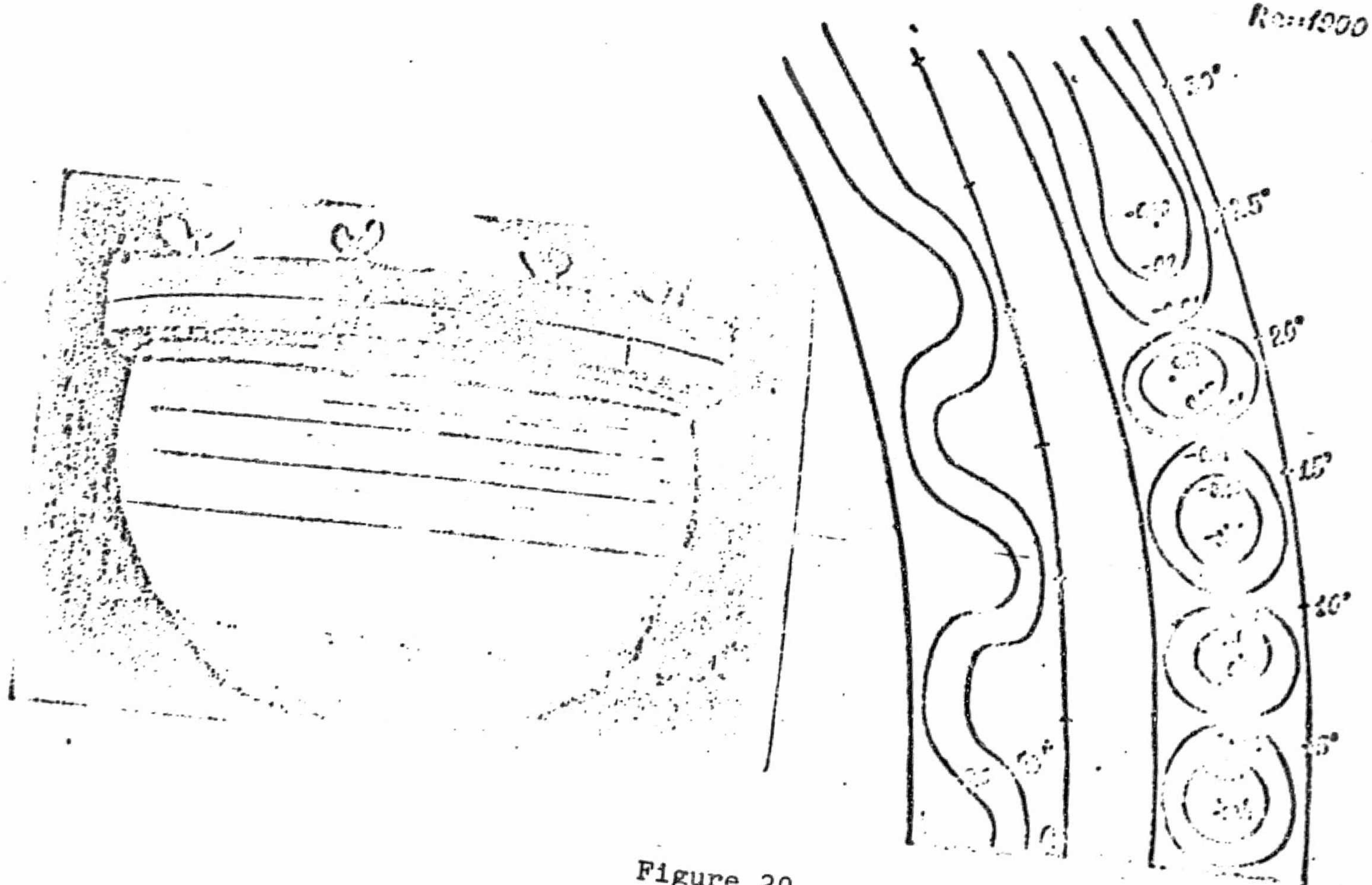

Figure 20

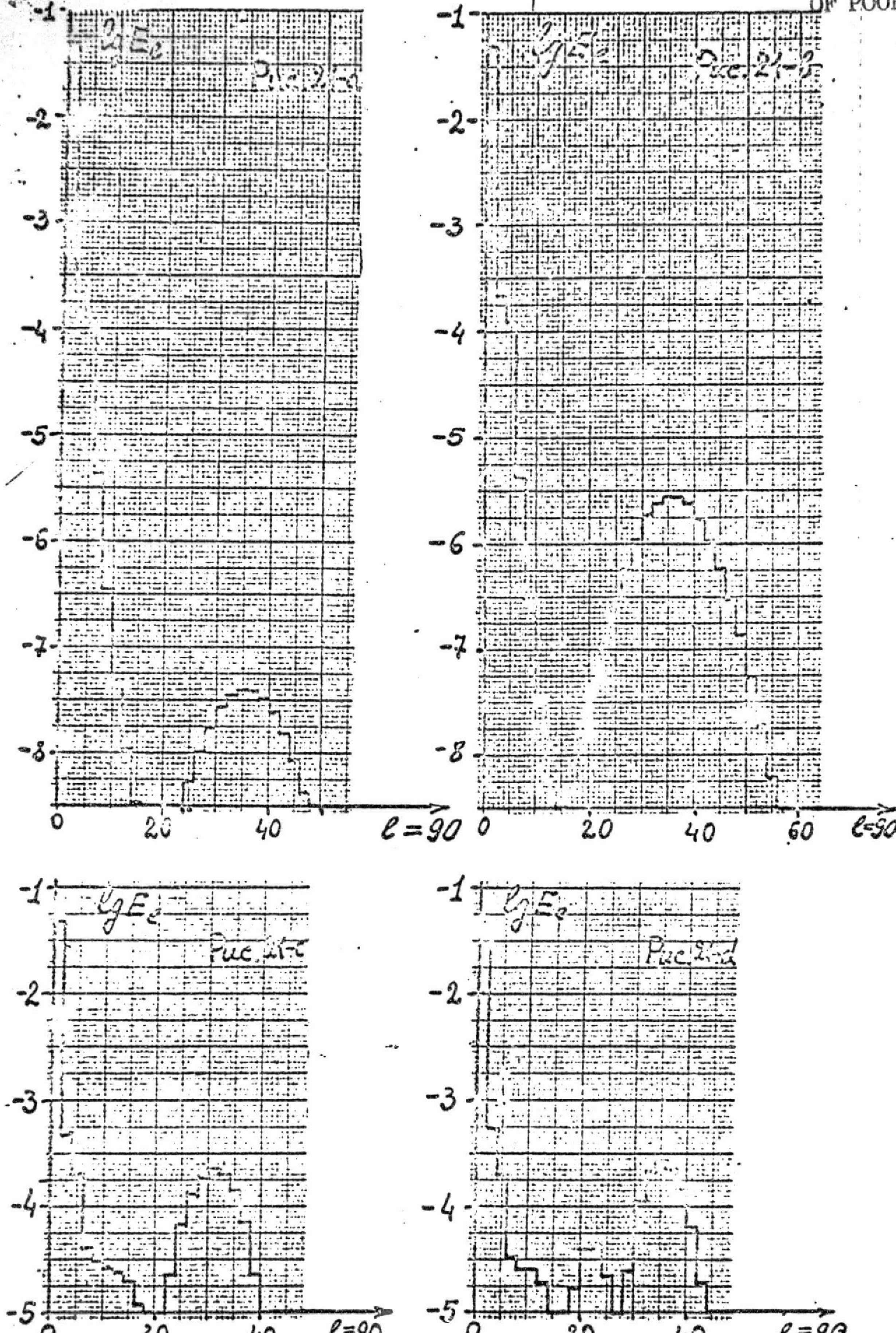

Figure 21

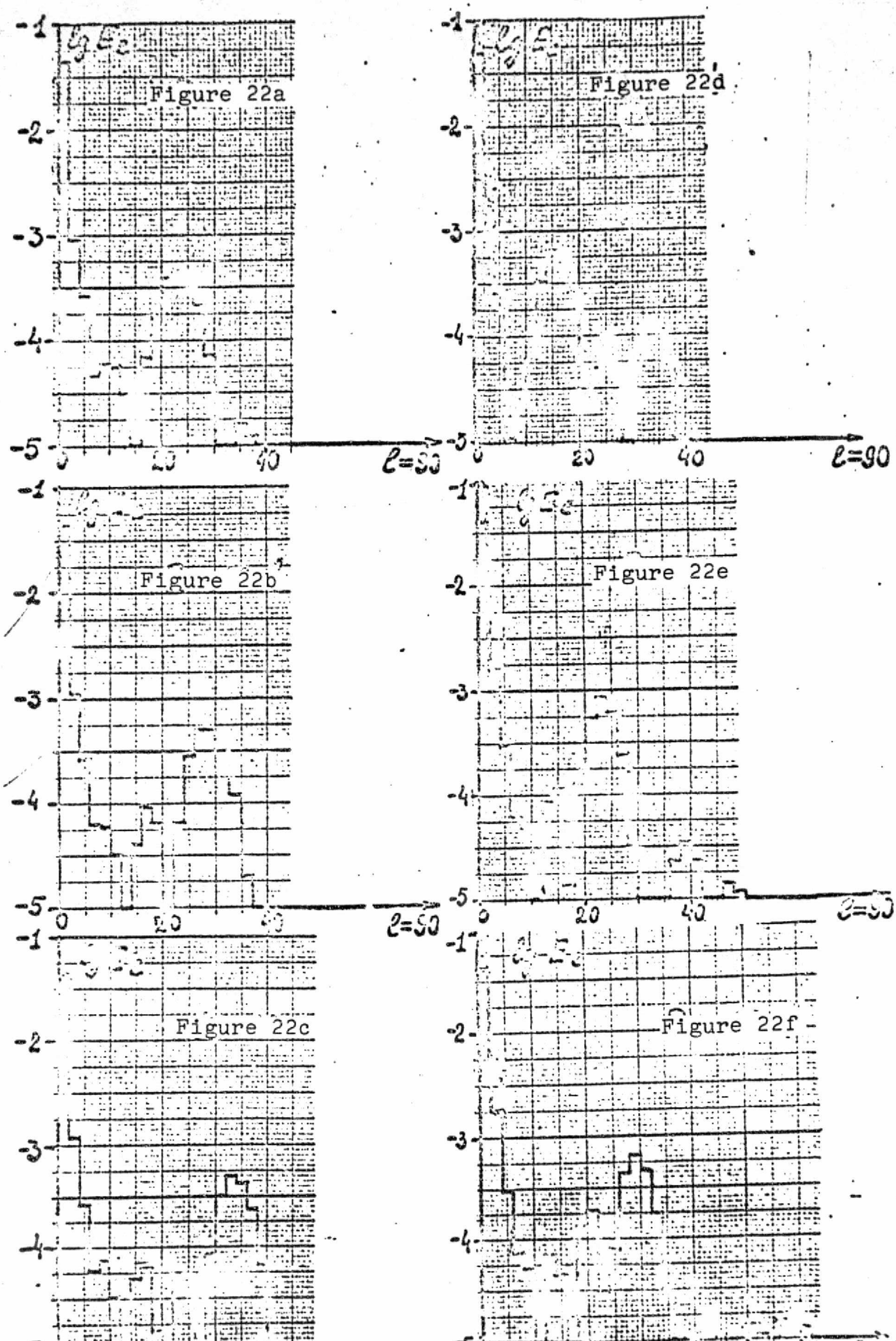
Figure 22a
Figure 22b
Figure 22c
Figure 22d
Figure 22e
Figure 22f
-1
-2
-3
-4
-5
0
20
40

Figure 22

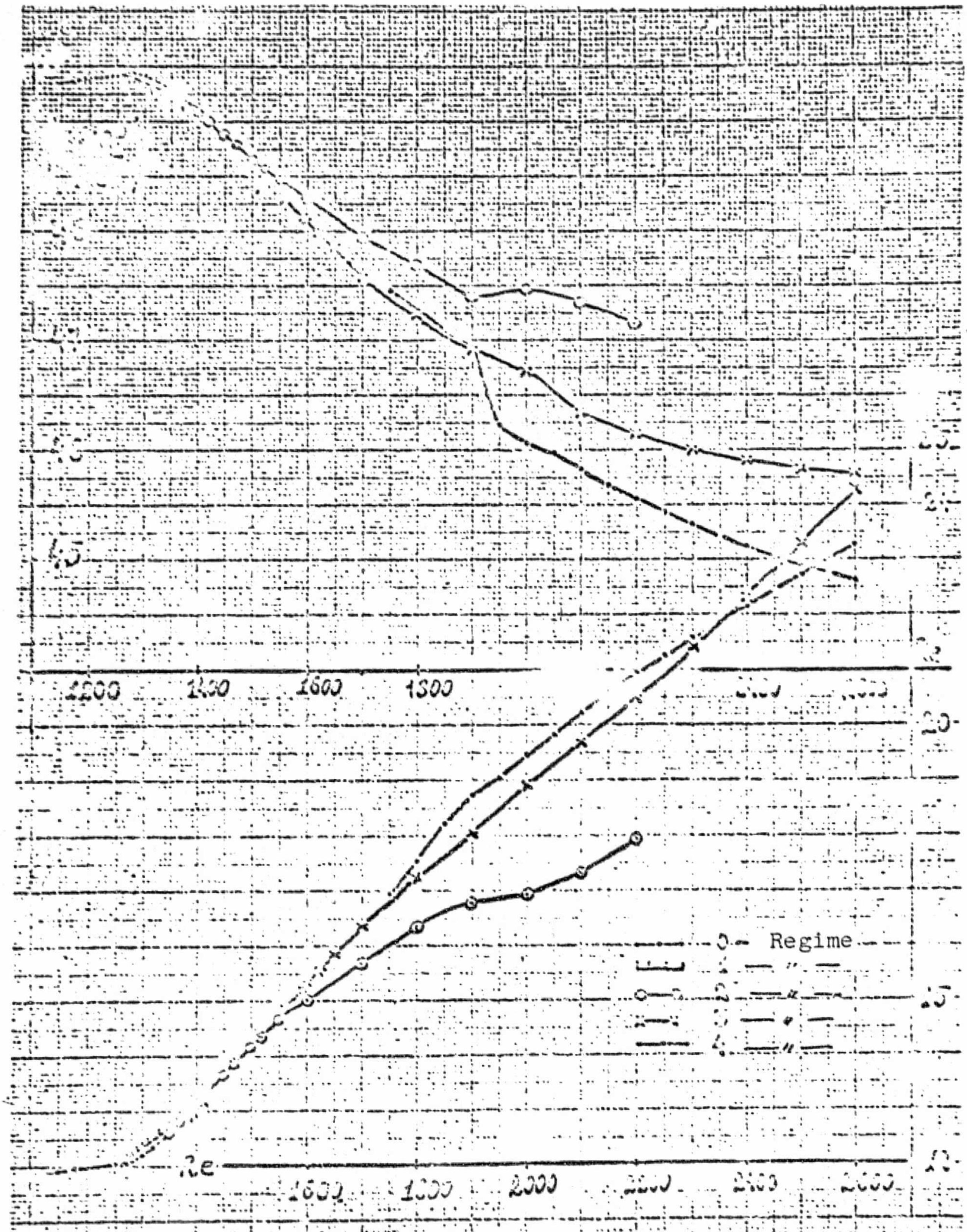

Figure 23